Received: 6 January 2024 | Revised: 6 March 2024 | Accepted: 29 March 2024

DOI: 10.1002/jbt.23706

RESEARCH ARTICLE

WILEY

# Novel diarylated tacrine derivatives: Synthesis, characterization, anticancer, antiepileptic, antibacterial, and antifungal activities

Büşra A. Mısır[1,2] | Yavuz Derin[1] | Salih Ökten[3] | Ali Aydın[4] | Ümit M. Koçyiğit[5] | Hatice Şahin[5] | Ahmet Tutar[1]

[1]Department of Chemistry, Faculty of Science, Sakarya University, Sakarya, Turkiye

[2]Department of Chemistry, Faculty of Science, Kahramanmaras Sütçü İmam University, Kahramanmaraş, Turkey

[3]Department of Maths and Science Education, Faculty of Education, Kırıkkale University, Kırıkkale, Turkiye

[4]Department of Basic Medical Science, Faculty of Medicine, Yozgat Bozok University, Yozgat, Turkiye

[5]Department of Basic Pharmaceutical Sciences, Sivas Cumhuriyet University, Sivas, Turkiye

**Correspondence**
Salih Ökten, Department of Maths and Science Education, Faculty of Education, Kırıkkale University, 71450, Yahşihan, Kırıkkale, Türkiye.
Email: salihokten@kku.edu.tr and sokten@gmail.com

**Funding information**
Turkish Health Institutes, Grant/Award Number: TUSEB A-Project No 24138; TUBITAK 2209-A Program, Grant/Award Number: 1919B012106356; Council of Higher Education (CoHE) of Turkey, Grant/Award Number: 100/2000

## Abstract

In this study, our goal was to synthesize novel aryl tacrine derivatives and assess their potential as anticancer, antibacterial agents, and enzyme inhibitors. We adopted a two-step approach, initiating with the synthesis of dibromotacrine derivatives **3** and **4** through the Friedlander reaction. These intermediates underwent further transformation into diarylated tacrine derivatives **3a–e** and **4a–e** using a Suzuki–Miyaura cross-coupling reaction. Thorough characterization of these novel diarylated tacrines was achieved using various spectroscopic techniques. Our findings highlighted the potent anticancer effects of these innovative compounds across a range of cancer cell lines, including lung, gynecologic, bone, colon, and breast cancers, while demonstrating low cytotoxicity against normal cells. Notably, these compounds surpassed the control drug, 5-Fluorouracil, in terms of antiproliferative activity in numerous cancer cell lines. Moreover, our investigation included an analysis of the inhibitory properties of these novel compounds against various microorganisms and cytosolic carbonic anhydrase enzymes. The results suggest their potential for further exploration as cancer-specific, enzyme inhibitory, and antibacterial therapeutic agents. Notably, four compounds, namely, 5,7-bis(4-(methylthio)phenyl)tacrine (**3d**), 5,7-bis(4-(trifluoromethoxy)phenyl)tacrine (**3e**), 2,4-bis(4-(trifluoromethoxy)phenyl)-7,8,9,10-tetrahydro-6H-cyclohepta[b]quinolin-11-amine (**4e**), and 6,8-dibromotacrine (**3**), emerged as the most promising candidates for preclinical studies.

**KEYWORDS**
antibacterial agents, anticancer agents, cytotoxicity, diarylated tacrine, enzyme inhibition, inducing apoptosis, Suzuki coupling

## 1 | INTRODUCTION

Heterocyclic compounds play a pivotal role in synthetic organic chemistry, material science, and pharmaceutical chemistry.[1–5] Compounds featuring fused quinoline, tetrahydroquinoline, and tetrahydroacridine motifs are particularly significant in the quest for new promising drugs.[6–12] Tacrine (9-amino-1,2,3,4-tetrahydroacridine), a heterocyclic compound containing a 1,2,3,4-tetrahydroacridine ring with an amino group, was the first drug approved by the US Food and Drug Administration for treating Alzheimer's disease. It is renowned as an acetylcholinesterase (AChE) inhibitor. However, this drug is no longer prescribed due to its severe side effects and hepatotoxicity.[13] Consequently, there is a high demand for new tacrine analogs with improved safety profiles and multitargeted properties, leading to the exploration of various synthetic strategies to obtain such compounds.[14] Many studies in the literature have reported that the use of tacrine derivatives as inhibitors of the AChE enzyme may also inhibit carbonic anhydrase enzymes, which play an effective role in the determination of many diseases (such as gastric and duodenal ulcers, glaucoma, mountain sickness, epilepsy, osteoporosis, and neurological disorders). In fact, our group's research on this subject has demonstrated the properties of tacrine derivatives as inhibitors of effective carbonic anhydrase enzymes.[15,16]

Tacrine, also known as tetrahydroaminoacridine, features a quinoline skeleton. Extensive research has been dedicated to exploring the antibacterial properties of quinoline derivatives, as documented in the literature. [6,17,18] Acridine derivatives were initially utilized as antibacterial and antiparasitic agents, with both natural and synthetic variants garnering significant interest among medicinal chemists as potential antibacterial and antitumor agents.[19] Ferguson and Thorne[20] reported that 5-aminoacridine exhibited antibacterial properties through increased medium basicity. Despite literature reports on the antibacterial properties of acridine compounds, research specifically targeting the antibacterial attributes of tacrine compounds, namely tetrahydroaminoacridine, remains relatively limited. Our group conducted a foundational study in this area, focusing on the antibacterial properties of tacrine derivatives. Through our investigation, we determined effective minimum inhibitory concentration (MIC) values against select Gram-positive and Gram-negative bacteria, thereby revealing the antibacterial potential inherent in tacrine derivatives.[7]

The Friedländer synthesis is a well-known methodology for producing various tacrine derivatives. This method involves the reaction between 2-aminobenzonitrile or its derivatives and cyclic ketones using various Lewis acids.[21] In this context, replacing 2-aminobenzonitrile with heterocyclic α-amino nitrile compounds leads to a wide variety of bioactive tacrine analogs with different heterocyclic moieties, such as pyrano[2,3-c]pyrazole,[22] 4-azaisoindole,[23,24] dihydropyridine,[25] 1,3-thiazolopyridine,[26] *4H*-pyran,[27] *4H*-pyrano[3,2-h]quinoline,[28] thiophene,[29] and more. Furthermore, the amino group in the tacrine core can be modified through various synthetic approaches, including reductive amination,[30] reaction with dihaloalkanes,[31] or acylchloride derivatives[32] and nucleophilic aromatic substitution reaction of 9-chloro-1,2,3,4 tacrine with amine compounds.[33] The Suzuki–Miyaura reaction is an exceptionally appealing method that involves the reaction of halogen-containing tacrines with (hetero)aromatic boronic acids or esters to enhance their bioactivity properties.[34,35] The Suzuki–Miyaura reaction is a cross-coupling reaction that forms C–C bonds between heteroaryl, aryl, alkenyl, or alkynyl organoboranes and organic halides or pseudohalides, catalyzed by a transition metal, often palladium, under basic conditions.[36,37] This coupling reaction is a versatile synthetic strategy for obtaining various bioactive molecules and important compounds across various research fields, thanks to its mild reaction conditions.[38]

In this study, as continuation of our previous works[6,21] and recent trend, 3,5-dibrom 2-aminobenzonitrile and cyclohexanone or cycloheptanone were annulated to dibromotacrine by Lewis acid catalysis, namely boron trifluoride. Dibromotacrines were cross-coupled with phenyl, 4-ethylphenyl, 4-metoxyphenyl, 4-thiomethylphenyl, and 4-trifluorophenyl boronic acids. Moreover, the anticancer potentials against A549, Calu1, SW1353, MG63, Saos2, HeLa, A2780, A2780ADR, SW620, HT29, and MCF7 cancer cell lines, and the enzyme inhibitory effects against cytosolic carbonic anhydrase (hCA I and hCA II) of diaryl substituted tacrine analogs were investigated using MTT (3-(4,5-dimethylthiazol-2-yl)-2,5-diphenyltetrazolium bromide), DNA laddering, lactate dehydrogenase (LDH) cytotoxicity, migration assays, and esterase method.

## 2 | MATERIALS AND METHODS

### 2.1 | Chemistry

#### 2.1.1 | General

All reagents and solvents used in the synthesis were commercially purchased from Sigma Aldrich and were used without further purification. The solvents employed in column chromatography were technical grade and were purified using standard methods before use.[39] Thin-layer chromatography (TLC) was conducted on Merck silica F254 plates with a thickness of 0.255 mm and spots were visualized under UV light at 254 nm. Nuclear magnetic resonance (NMR) spectra ($^{1}$H, $^{13}$C, and $^{19}$F) were acquired in $CDCl_3$ using a Varian Infinity Plus spectrometer, operating at 300 MHz for $^{1}$H NMR, 75 MHz for $^{13}$C NMR, and 282 MHz for $^{19}$F NMR. High-resolution electrospray ionization (ESI) mass spectra were obtained using a Waters SYNAPT MS series system. Melting points of the synthesized compounds were determined using a Schorpp MPM-H1 device. Infrared (IR) spectra were recorded using a Perkin Elmer Spectrum Two Fourier-transform IR (FT-IR) (ATR) instrument.

#### 2.1.2 | Synthesis of 3,5-dibromo-2-aminobenzonitrile (2)

The bromination reaction was carried out following a procedure described in the literature.[21] In a double-necked round-bottom flask

(100 mL), 2-aminobenzonitrile (1.18 g, 0.01 mol) was dissolved in 5 mL of glacial acetic acid. While maintaining the reaction mixture at a temperature of 10–15°C, a solution of $Br_2$ (3.2 g, 0.02 mmol) in acetic acid (10 mL) was added slowly over a period of 15–20 min using a pressure-balanced dropping funnel. After the addition of the $Br_2$ solution, the reaction was allowed to proceed for 5 h. The resulting reaction mixture was poured into an ice–water mixture, resulting in the formation of a white precipitate. This precipitate was then filtered and washed with 150 mL of water. The resulting white solid was subsequently dried in an oven at a temperature of 75–80°C, yielding a product with a 98% yield. $^1$H NMR (300 MHz, $CDCl_3$, ppm): $\delta$ 7.73 (d, $J$ = 2.2 Hz, 1H, ArH)), 7.48 (d, $J$ = 2.2 Hz, 1H, ArH), 4.90 (brs, 2H, $NH_2$). $^{13}$C NMR (75 MHz, $CDCl_3$, ppm): $\delta$ 148.87, 137.26, 134.39, 117.05, 116.54, 108.94, 97.74.

### 2.1.3 | Synthesis of tacrine derivatives (3 and 4)

Both brominated tacrine derivatives (**3** and **4**) were synthesized following the procedure described in the literature.[21] In a 50 mL double-necked round-bottom flask equipped with a reflux condenser, 2-amine-3,5-dibromobenzonitrile (**2**) (0.55 g, 2 mmol), cyclohexanone (0.22 g, 2.2 mmol), and boron trifluoride diethyl etherate ($BF_3{\cdot}OEt_2$) (0.30 mL, 2.4 mmol) were combined in 12 mL of toluene. The mixture was stirred at 120°C for 24 h. After cooling to room temperature, the remaining solid was treated with a 2 M NaOH solution (10 mL) and the resulting mixture was refluxed for an additional 24 h. The reaction was considered complete and the mixture was extracted with $CHCl_3$ (3 × 40 mL). The organic phase was then dried over $Na_2SO_4$. Afterward, the organic layers were concentrated using an evaporator, resulting in the isolation of yellow crystals (compound **3**) with a yield of 58%.$^1$H NMR (300 MHz, $CDCl_3$, ppm): $\delta$ 7.93 (d, $J$ = 2.0 Hz, 1H, ArH), 7.78 (d, $J$ = 2.0 Hz, 1H, ArH), 4.74 (brs, 2H, $NH_2$), 3.01 (t, $J$ = 5.8 Hz, 2H, $CH_2$), 2.53 (t, $J$ = 6.0 Hz, 2H, $CH_2$), 1.88–1.82 (m, 4H, $2CH_2$). $^{13}$C NMR (75 MHz, $CDCl_3$, ppm): $\delta$ 160.58, 146.26, 142.59, 134.86, 126.00, 122.58, 119.31, 116.43, 112.33, 34.59, 24.03, 22.98, 22.83.

In a 50 mL double-necked round-bottom flask equipped with a reflux condenser, 2-amine-3,5-dibromobenzonitrile (**2**) (0.55 g, 2 mmol), cycloheptanone (0.24 g, 2.19 mmol), and boron trifluoride diethyl etherate ($BF_3{\cdot}OEt_2$) (0.30 mL, 2.4 mmol) were combined in 12 mL of toluene. The mixture was stirred at 120°C for 24 h. After cooling to room temperature, the remaining solid was treated with a 2 M NaOH solution (10 mL), and the resulting mixture was refluxed for an additional 24 h. The reaction was considered complete and the mixture was extracted with $CHCl_3$ (3 × 40 mL). The organic phase was then dried over $Na_2SO_4$. Subsequently, the organic layers were concentrated using an evaporator, resulting in the isolation of yellow crystals (Compound **4**) with a yield of 20%. $^1$H NMR (300 MHz, $CDCl_3$, ppm): $\delta$ 7.98 (d, $J$ = 2.0 Hz, 1H, ArH), 7.80 (d, $J$ = 2.0 Hz, 1H, ArH), 3.16 (t, $J$ = 6.0 Hz, 2H, $CH_2$), 2.73 (t, $J$ = 6.0 Hz, 2H, $CH_2$), 1.89–1.71 (m, 6H, $3CH_2$). $^{13}$C NMR (75 MHz, $CDCl_3$, ppm): $\delta$ 166.54, 144.79, 142.35, 134.76, 126.01, 123.12, 120.17, 117.80, 117.07, 40.31, 32.23, 27.57, 27.06, 26.88.

### 2.1.4 | General method of Suzuki coupling for synthesis of diarylated tacrines (**3a–e** and **4a–e**)

The brominated tacrine derivatives (**3** and **4**) (1.0 eq) and 1,4-dioxane (15 mL) were introduced into a three-necked round-bottom flask equipped with a reflux condenser at room temperature, under a nitrogen atmosphere. Once the mixture was completely dissolved, arylboronic acid (2.6 eq), Pd ($PPh_3$)$_4$ (0.05 eq), and a solution of $K_2CO_3$ (3 M, 15 mL) were added to the reaction flask, and the mixture was refluxed at 120°C for 6 h. The progress of the reaction was monitored using TLC. Upon completion of the reaction, the mixture was extracted with $CHCl_3$ (3 × 20 mL). The organic layers were combined and dried over $Na_2SO_4$. The filtrate was concentrated under reduced pressure and the residue was purified by column chromatography (using silica gel and $CHCl_3$/MeOH as the eluent) to obtain the desired products.

*5,7-Diphenyl-1,2,3,4-tetrahydroacridine-9-amine (**3a**)*

Compound **3a** was synthesized by mixing 5,7-dibromo-1,2,3,4-tetrahydroacridin-9-amine (**3**) (0.2 g, 0.56 mmol), phenylboronic acid (0.18 g, 1.46 mmol), Pd($PPh_3$)$_4$ (0.032 g, 0.028 mmol), and $K_2CO_3$ solution. Yellow powder solid (0.1 g, 51%). Mp 209–210°C.$^1$H NMR (300 MHz, $CDCl_3$) $\delta$ 7.94 (s, 1H), 7.85 (s, 1H), 7.74 (dd, $J$ = 10.1, 7.4 Hz, 4H), 7.51–7.33 (m, 6H), 5.03 (s, 2H), 2.92 (t, $J$ = 5.9 Hz, 2H), 2.59 (t, $J$ = 6.1 Hz, 2H), 1.88 (m, 2H). $^{13}$C NMR (75 MHz, $CDCl_3$) $\delta$ 158.60, 147.46, 143.83, 141.22, 140.76, 140.33, 136.06, 131.44, 129.45, 129.11, 128.00, 127.51, 127.47, 127.28, 118.26, 118.07, 110.82, 34.64, 24.02, 23.16. FT-IR (neat $\tilde{\nu}$ cm$^{-1}$) 3483 ($NH_2$), 2936–2861 (Aliph. C–H), 1632, 1560 (C=N), 1482, 755, 697. High-resolution mass spectrometry (HRMS) (ESI) $m/z$: calcd. for $C_{25}H_{22}N_2$ $[M + H]^+$: 351.1861, Found: 351.1870.

*5,7-Bis(4-ethylphenyl)-1,2,3,4-tetrahydroacridine-9-amine (**3b**)*

Compound **3b** was synthesized by mixing 5,7-dibromo-1,2,3,4-tetrahydroacridine-9-amine (**3**) (0.21 g, 0.59 mmol), 4-(ethylphenyl) boronic acid (0.23 g, 1.53 mmol), Pd($PPh_3$)$_4$ (0.034 g, 0.029 mmol), and $K_2CO_3$ solution. Yellow powder solid (0.15 g, 63%). Mp 182–183°C. $^1$H NMR (300 MHz, $CDCl_3$) $\delta$ 8.12 (s, 1H), 7.85 (s, $J$ = 1.7 Hz, 1H), 7.70 (d, $J$ = 8.2 Hz, 2H), 7.61 (d, $J$ = 7.8 Hz, 2H), 7.31 (d, $J$ = 8.1 Hz, 4H), 2.89 (t, $J$ = 5.8 Hz, 2H), 2.79–2.66 (m, 2H), 2.55 (t, $J$ = 5.3 Hz, 2H), 1.84–1.72 (m, 4H), 1.30 (q, $J$ = 7.6 Hz, 3H). $^{13}$C NMR (75 MHz, $CDCl_3$) $\delta$ 157.87, 147.63, 143.60, 143.26, 139.86, 138.55, 137.77, 136.16, 132.29, 131.25, 129.38, 128.64, 127.58, 127.45, 118.17, 117.57, 110.65, 34.40, 28.95, 28.85, 23.98, 23.10, 15.98, 15.78. FT-IR (neat $\tilde{\nu}$ cm$^{-1}$) 3452 ($NH_2$), 2961–2870 (Aliph. C–H), 1635 (C=N), 1482–1435, 1116, 827, 722. HRMS (ESI) $m/z$: calcd. for $C_{29}H_{30}N_2$ $[M + H]^+$: 407.2487, Found: 407.2482.

*5,7-Bis(4-methoxyphenyl)-1,2,3,4-tetrahydroacridine-9-amine (**3c**)*

Compound **3c** was synthesized by mixing 5,7-dibromo-1,2,3,4-tetrahydroacridin-9-amine (**3**) (0.21 g, 0.59 mmol), 4-(methoxyphenyl) boronic acid (0.23 g, 1.53 mmol), Pd($PPh_3$)$_4$ (0.034 g, 0.029 mmol), and $K_2CO_3$ solution. Yellow powder solid (0.14 g, 58%). Mp 170–171°C. $^1$H NMR (300 MHz, $CDCl_3$) $\delta$ 8.95 (s, 2H), 7.93 (d, $J$ = 8.6 Hz, 2H), 7.81 (s, 1H), 7.45 (d, $J$ = 8.6 Hz, 2H), 7.08 (d, $J$ = 8.6 Hz, 2H), 6.99 (d, $J$ = 8.7 Hz, 2H), 3.89 (s, 3H), 3.82 (s, 3H), 2.87 (t,

$J$ = 5.6 Hz, 2H), 2.58 (t, $J$ = 6.9 Hz, 2H), 1.95–1.65 (m, 4H). $^{13}$C NMR (75 MHz, $CDCl_3$) $\delta$ 159.33, 159.10, 157.83, 147.99, 143.33, 139.49, 135.67, 133.52, 133.13, 132.39, 129.02, 128.42, 118.31, 117.17, 114.52, 113.51, 110.60, 55.63, 55.52, 34.37, 23.93, 23.12. FT-IR (neat $\tilde{\nu}$ cm$^{-1}$) 3330 ($NH_2$), 2920–2847 (Aliph. C–H), 1651,1604, 1513 (C=N), 1485, 1246, 1177, 1030, 830. HRMS (ESI) $m/z$: calcd. for $C_{27}H_{26}N_2O_2$ $[M + H]^+$: 411.2073, Found: 411.2081.

*5,7-Bis(4-(methylthio)phenyl)-1,2,3,4 tetrahydroacridine-9-amine (**3d**)*

Compound **3c** was synthesized by mixing 5,7-dibromo-1,2,3,4-tetrahydroacridin-9-amine (**3**) (0.4 g, 1.12 mmol), 4-(methylthiophenyl) boronic acid (0.49 g, 2.92 mmol), $Pd(PPh_3)_4$ (0.064 g, 0.056 mmol), and $K_2CO_3$ solution. Yellow powder solid (0.31 g, 63%). Mp 131–132°C. $^1$H NMR (300 MHz, $CDCl_3$) $\delta$ 7.95 (s, 1H), 7.78 (s, $J$ = 1.9 Hz, 1H), 7.66 (dd, $J$ = 13.1, 8.3 Hz, 4H), 7.32 (dd, $J$ = 18.8, 10.5 Hz, 4H), 2.92 (t, $J$ = 5.4 Hz, 2H), 2.63–2.56 (m, 2H), 2.54 (s, $J$ = 1.3 Hz, 3H), 2.52 (s, $J$ = 1.2 Hz, 3H), 1.90 (m, 4H). $^{13}$C NMR (75 MHz, $CDCl_3$) $\delta$ 158.50, 147.15, 143.68, 139.67, 137.93, 137.71, 137.32, 135.42, 131.71, 128.72, 127.74, 127.10, 126.13, 118.22, 117.43, 110.89, 34.58, 24.00, 23.11, 16.17. FT-IR (neat $\tilde{\nu}$ cm$^{-1}$) 3461 ($NH_2$), 2934–2859 (Aliph. C–H), 1637, 1479 (C=N), 813. HRMS (ESI) $m/z$: calcd. for $C_{27}H_{26}N_2S_2$ $[M + H]^+$: 443.1616, Found: 443.1656.

*5,7-Bis(4-(trifluoromethoxy)phenyl)-1,2,3,4-tetrahydroacridine-9-amine (**3e**)*

Compound **3e** was synthesized by mixing 5,7-dibromo-1,2,3,4-tetrahydroacridin-9-amine (**3**) (0.37 g, 1.039 mmol), 4-(trifluoromethoxyphenyl)boronic acid (0.56 g, 2.70 mmol), $Pd(PPh_3)_4$ (0.060 g, 0.052 mmol), and $K_2CO_3$ solution. Yellow powder solid (0.36 g, 67%). Mp 131–132°C. $^1$H NMR (300 MHz, $CDCl_3$) $\delta$ 8.06 (d, $J$ = 9.0 Hz, 2H), 7.85 (s, 1H), 7.60 (d, $J$ = 8.9 Hz, 2H), 7.45 (d, $J$ = 7.8 Hz, 2H), 7.31 (d, $J$ = 8.0 Hz, 2H), 2.88 (t, $J$ = 9.9 Hz, 2H), 2.62 (t, $J$ = 5.8 Hz, 2H), 1.90–1.65 (m, 4H). $^{13}$C NMR (75 MHz, $CDCl_3$) $\delta$ 159.16, 148.87, 148.68, 147.15, 143.75, 139.85, 139.13, 138.88, 134.79, 132.59, 132.35, 132.22, 129.02, 128.87, 128.77, 128.71, 122.56, 122.49, 121.50, 120.28, 119.15, 119.08, 118.32, 118.20, 111.13, 34.61, 23.97, 23.03. $^{19}$F NMR (282 MHz, $CDCl_3$) $\delta$ −58.02, −58.20. FT-IR (neat $\tilde{\nu}$ cm$^{-1}$) 3483 ($NH_2$), 2936–2861 (Aliph. C–H), 1485 (C=N), 1249–1152 (C-F). HRMS (ESI) $m/z$: calcd. for $C_{27}H_{20}F_6N_2O_2$ $[M + H]^+$: 519.1507, Found: 519.1533.

*2,4-Diphenyl-7,8,9,10-tetrahydro-6H-cyclohepta[b]quinolin-11-amine (**4a**)*

Compound **4a** was synthesized by mixing 2,4-dibromo-7,8,9,10-tetrahydro-6H-cyclohepta[b]quinolin-11-amine (**4**) (0.31 g, 0.84 mmol), phenylboronic acid (0.26 g, 2.18 mmol), $Pd(PPh_3)_4$ (0.048 g, 0.042 mmol), and $K_2CO_3$ solution. Yellow powder solid (0.18 g, 60%). Mp 134–135°C. $^1$H NMR (300 MHz, $CDCl_3$) $\delta$ 7.87 (s, 1H), 7.83 (d, $J$ = 6.9 Hz, 2H), 7.72 (d, $J$ = 7.0 Hz, 2H), 7.54–7.33 (m, 7H), 4.76 (bs, 2H), 3.13–3.02 (m, 2H), 2.82–2.68 (m, 2H), 1.87 (dd, $J$ = 10.2, 5.2 Hz, 2H), 1.72 (dd, $J$ = 15.6, 11.0 Hz, 4H). $^{13}$C NMR (75 MHz, $CDCl_3$) $\delta$ 164.46, 146.17, 143.06, 141.24, 140.35, 136.81, 133.30, 132.39, 132.26, 131.33, 129.43, 129.11, 128.89, 128.73, 127.99, 127.62, 127.53, 127.31, 118.96, 118.60, 116.28, 40.19, 32.43, 27.85, 27.28, 26.79. FT-IR (neat $\tilde{\nu}$ cm$^{-1}$) 3472 ($NH_2$), 2953–2847 (Aliph. C–H), 1629 (C=N), 1479, 752, 694. HRMS (ESI) $m/z$: calcd. for $C_{26}H_{24}N_2$ $[M + H]^+$: 365.2018, Found: 365.2024.

*2,4-Bis(4-ethylphenyl)-7,8,9,10-tetrahydro-6H-cyclohepta[b]quinolin-11-amine (**4b**)*

Compound **4b** was synthesized by mixing 2,4-dibromo-7,8,9,10-tetrahdro-6H-cyclohepta[b]quinolin-11-amine (**4**) (0.32 g, 0.86 mmol), 4-(ethylphenyl)boronic acid (0.34 g, 2.25 mmol), $Pd(PPh_3)_4$ (0.050 g, 0.043 mmol), and $K_2CO_3$ solution. Yellow powder solid (0.22 g, 61%). Mp 105–108°C. $^1$H NMR (300 MHz, $CDCl_3$) $\delta$ 7.92 (s, 1H), 7.89 (s, $J$ = 8.7 Hz, 1H), 7.80–7.70 (m, 2H), 7.72–7.64 (m, 2H), 7.60–7.52 (m, 2H), 7.54–7.43 (m, 2H), 7.36–7.27 (m, 3H), 5.04 (s, 2H), 3.11–3.01 (m, 2H), 2.81–2.69 (m, 4H), 1.92–1.80 (m, 4H), 1.78–1.61 (m, 2H), 1.39–1.24 (m, 3H).$^{13}$C NMR (75 MHz, $CDCl_3$) $\delta$ 164.51, 155.72, 146.44, 143.71, 143.31, 140.72, 138.93, 138.31, 136.83, 132.57, 131.54, 129.44, 129.14, 128.98, 128.85, 128.75, 127.75, 127.36, 119.34, 118.41, 116.24, 40.44, 32.64, 28.09, 27.55, 26.89, 16.23, 16.08. FT-IR (neat $\tilde{\nu}$ cm$^{-1}$) 3452 ($NH_2$), 2961–2850 (Aliph. C–H), 1632 (C=N), 1479, 821. HRMS (ESI) $m/z$: calcd. for $C_{30}H_{32}N_2$ $[M + H]^+$: 421.2644, Found: 421.2684.

*2,4-Bis(4-methoxyphenyl)-7,8,9,10-tetrahydro-6H-cyclohepta[b]quinolin-11-amine (**4c**)*

Compound **4c** was synthesized by mixing 2,4-dibromo-7,8,9,10-tetrahdro-6H-cyclohepta[b]quinolin-11-amine (**4**) (0.25 g, 0.675 mmol), 4-(methoxyphenyl)boronic acid (0.27 g, 1.756 mmol), $Pd(PPh_3)_4$ (0.039 g, 0.034 mmol), and $K_2CO_3$ solution. Yellow powder solid (0.16 g, 55%). Mp 125–128°C. $^1$H NMR (300 MHz, $CDCl_3$) $\delta$ 7.87–7.74 (m, 4H), 7.64 (d, $J$ = 8.7 Hz, 2H), 7.11–6.96 (m, 4H), 4.82 (bs, 2H), 3.87 (s, 3H), 3.86 (s, 3H), 3.16–3.03 (m, 2H), 2.84–2.65 (m, 2H), 1.95–1.81 (m, 2H), 1.80–1.65 (m, 4H). $^{13}$C NMR (75 MHz, $CDCl_3$) $\delta$ 164.01, 159.36, 159.08, 146.00, 143.05, 139.95, 136.40, 133.88, 132.95, 132.45, 128.91, 128.61, 119.10, 117.44, 116.19, 114.53, 113.48, 55.63, 40.35, 32.46, 27.89, 27.37, 26.79. FT-IR (neat $\tilde{\nu}$ cm$^{-1}$) 3475 ($NH_2$), 2919–2832 (Aliph. C–H), 1633 (C=N), 1511, 1480, 1243, 1174, 1030, 824. HRMS (ESI) $m/z$: calcd. for $C_{28}H_{28}N_2O_2$ $[M + H]^+$: 425.2229, Found: 425.2272.

*2,4-Bis(4-(methylthio)phenyl)-7,8,9,10-tetrahydro-6H-cyclohepta[b]quinolin-11-amine (**4d**)*

Compound **4d** was synthesized by mixing 2,4-dibromo-7,8,9,10-tetrahdro-6H-cyclohepta[b]quinolin-11-amine (**4**) (0.24 g, 0.65 mmol), 4-(methylthiophenyl) boronic acid (0.28 g, 1.69 mmol), $Pd(PPh_3)_4$ (0.036 g, 0.033 mmol), and $K_2CO_3$ solution. Yellow powder solid (0.23 g, 78%). Mp 184–186°C. $^1$H NMR (300 MHz, $CDCl_3$) $\delta$ 7.82 (s, 1H), 7.76 (d, $J$ = 7.9 Hz, 2H), 7.65 (d, $J$ = 8.3 Hz, 2H), 7.37 (dd, $J$ = 8.4, 1.1 Hz, 4H), 4.65 (s, 2H), 3.13–2.99 (m, 2H), 2.82–2.71 (m, 2H), 2.55 (s, 3H), 2.54 (s, 3H), 1.95–1.81 (m, 2H), 1.79–1.64 (m, 4H). $^{13}$C NMR (75 MHz, $CDCl_3$) $\delta$ 164.56, 145.41, 143.34, 140.08, 138.11, 137.90, 137.31, 137.17, 136.22, 131.74, 128.68, 127.90, 127.17, 126.20, 119.04, 117.76, 116.52, 40.44, 32.42, 27.89, 27.33, 26.87, 16.22, 16.14. FT-IR (neat $\tilde{\nu}$ cm$^{-1}$) 3366 ($NH_2$), 2920–2847 (Aliph. C–H), 1657 (C=N), 1482, 1421, 1368, 813. HRMS (ESI) $m/z$: calcd. for $C_{28}H_{28}N_2S_2$ $[M + H]^+$: 457.1772, Found: 457.1760.

*2,4-Bis(4-(trifluoromethoxy)phenyl)-7,8,9,10-tetrahydro-6H-cyclohepta[b]quinolin-11-amine (**4e**)*

Compound **4e** was synthesized by mixing 2,4-dibromo-7,8,9,10-tetrahdro-6H-cyclohepta[b]quinolin-11-amine (**4**) (0.26 g, 0.70 mmol),

4-(trifluoromethoxyphenyl) boronic acid (0.37 g, 1.83 mmol), Pd $(PPh_3)_4$ (0.040 g, 0.035 mmol), and $K_2CO_3$ solution. Light gray powder solid (0.23 g, 62%). Mp 100–102°C. $^1$H NMR (300 MHz, $CDCl_3$) $\delta$ 7.85 (d, $J$ = 8.7 Hz, 2H), 7.79 (s, $J$ = 1.9 Hz, 1H), 7.71 (d, $J$ = 8.6 Hz, 2H), 7.36–7.27 (m, 4H), 4.73 (s, 2H), 3.12–3.00 (m, 2H), 2.83–2.72 (m, 2H), 1.94–1.84 (m, 2H), 1.81–1.62 (m, 4H). $^{13}$C NMR (75 MHz, $CDCl_3$) $\delta$ 165.25, 148.93, 148.71, 145.69, 143.43, 139.91, 139.45, 138.88, 135.41, 132.65, 128.97, 128.85, 122.59, 122.53, 121.56, 120.33, 119.18, 119.12, 119.06, 118.83, 116.73, 40.37, 32.36, 27.77, 27.26, 26.76. $^{19}$F NMR (282 MHz, $CDCl_3$) $\delta$ −58.00, −58.21. FT-IR (neat $\nu^{\sim}$ $cm^{-1}$) 3491 ($NH_2$), 2922–2853 (Aliph. C–H), 1629 (C=N), 1482, 1249- 1152 (C–F). HRMS (ESI) $m/z$: calcd. for $C_{28}H_{22}F_6N_2O_2$ $[M + H]^+$: 533.1664, Found: 533.1681.

## 2.2 | Anticancer and hCA enzymes inhibition studies

### 2.2.1 | Cancer cell lines and cell culture

In this study, we employed various cancer cell lines, including A549 (ATCC, CCL-185) and Calu1 (ATCC, HTB-54) lung cancer cell lines, SW1353 (ATCC, HTB-94), MG63 (ATCC, CRL-1427), and Saos2 (ATCC, HTB-85) bone cancer cell lines, HeLa (ATCC, CCL-2), A2780 (RRID, CVCL-0134), and A2780ADR (RRID CVCL-1941) gynecological cancer cell lines, SW620 (ATCC, CCL-227) and HT29 (ATCC, HTB-38) colon cancer cell lines, MCF7 (ATCC, HTB-22) breast cancer cell line, as well as the Beas2B (RRID, CVCL-0168) normal lung cell line, HC (Sigma Aldrich, 402-05A) normal chondrocytes cell line, and FL (ATCC, CCL-62) normal amnion cell line.

All cell preparation procedures were conducted in a sterile environment within a laminar cabinet. The cell lines were used once they reached confluence under conditions of 37°C and 5% $CO_2$ in supplemented Dulbecco's modified Eagle medium or RPMI 1640 medium containing 10% fetal bovine serum and 2% PenStrep solution. Cells were seeded at a density of 10,000 cells per well on measuring plates. After ~16 h of pre-incubation, test molecules were introduced and measurements were conducted following 24 h of incubation.

### 2.2.2 | Cell proliferation measurement and determination of NCI-60 survival parameters

The MTT assay was utilized to assess the impact of the synthesized test compounds on cell proliferation and determine NCI-60 survival parameter values.[40] This test protocol was applied following a 24 h incubation of the test substances with the cancer cell lines. The results were reported as % cell inhibition, with the optical density of the solvent (dimethyl sulfoxide [DMSO])-treated cells considered as 100%.

The MTT method involved testing cells at increasing concentrations of each test substance (1.96, 3.91, 7.81, 15.63, 31.25, 62.5, and 125.0 μg/mL) across a specified range to ascertain the NCI-60 survival parameters of the test substances. The analysis was conducted by fitting the data to a logarithmic function using the absorbance values obtained. The following formulas were employed to determine the NCI-60 survival parameters ($GI_{50}$, total growth inhibition [TGI], and $LC_{50}$):

Cell proliferation: $[(Ti - Tz)/(C - Tz)] \times 100$, if $Ti \geq Tz$ (indicating a cytocytic effect), or $[(Ti - Tz)/Tz] \times 100$, if $Ti < Tz$ (indicating a cytocidal or cytotoxic effect) (Tz; zero point, C; control growth, Ti; inhibition by the test substance).

$GI_{50}$ : Concentration value that reduces growth by 50% ($[(Ti - Tz)/(C - Tz)] \times 100 = 50$).

TGI: Concentration value that reduces growth by 100% ($Ti = Tz$).

$LC_{50}$ : Concentration value that kills 50% of cells in the medium ($[(Ti - Tz)/Tz] \times 100 = -50$).

### 2.2.3 | Cytotoxicity test

The determination of whether the test substances exhibited cytotoxic or cytostatic effects was carried out using the LDH method.[41] An increase in the number of cells that die during the incubation period, due to the tested substance, results in a corresponding increase in LDH levels in the culture supernatant. LDH is a stable cytoplasmic enzyme found in most cells.

For this purpose, the LDH cell cytotoxicity kit was employed, following the manufacturer's instructions. In brief, the change in the amount of formazan formed as a result of LDH enzyme activity was measured and evaluated using the formula below:

$$\%\ \text{Cytotoxicity} = [(\text{Substance absorbance} - \text{Low control}) / (\text{High control} - \text{Low control}) \times 100].$$

This formula allowed the quantification of cytotoxicity, with the absorbance values of the low control and high control used as reference points for the calculation.

### 2.2.4 | Measurement of mitochondrial membrane potential

The mitochondrial membrane potential was assessed through inverted-phase-contrast microscopy using the fluorescent dye Rhodamine 123.[42] The experimental procedure involved the following steps:

1. Cells were seeded into 24-well plates.
2. The cells were exposed to the test substances for a duration of 24 h.
3. After the incubation period, the cells were rinsed three times with phosphate-buffered saline (PBS).

4. Subsequently, the cells were incubated with a 5 μg/mL solution of Rhodamine 123 for 30 min at 37°C in a humidified atmosphere, while being kept in the dark.
5. The plate was gently washed three times with PBS to remove excess dye.
6. Finally, images of the cells were captured using an inverted-phase-contrast microscope.

This process allowed for the evaluation of mitochondrial membrane potential based on the fluorescence of Rhodamine 123 within the cells.

### 2.2.5 | DNA fragmentation by agarose gel electrophoresis

The DNA laddering activity of the compounds was assessed using a DNA laddering assay following the standard method.[43] Here's a summary of the procedure:

1. A total of $7.5 \times 10^5$ cells were placed into 25 $cm^2$ culture flasks.
2. These cells were treated with the TGI concentrations of the compounds.
3. The treatment was carried out at 37°C with 5% $CO_2$ overnight.

The subsequent steps involve the DNA extraction and analysis:

1. DNA-containing precipitate was extracted from the digest by adding a 50 μL phosphate-citrate buffer and then centrifuging the mixture at 1500*g* for 5 min.
2. Subsequently, 40 μL of the supernatant was carefully transferred to a microcentrifuge tube.
3. To this supernatant, a Tween20 solution (5 μL) at a concentration of 0.25% in dd$H_2O$ was added, along with an RNase A solution (5 μL).
4. The mixture was incubated at 37°C for 30 min.
5. Following this incubation, proteinase K (5 μL) was introduced to each tube and the samples were re-incubated at 37°C for 5 min.
6. The DNA-containing precipitate from the microcentrifuge tube was then combined with 5 μL of loading buffer.
7. This mixture was loaded onto a 1.5% agarose gel that contained 0.5 μg/mL ethidium bromide.
8. Electrophoresis was performed at 200 mA for 40 min.
9. After electrophoresis, the DNA fragmentation on the gel was visualized using a UVP gel imaging system.

The DNA laddering assay allows for the detection of DNA fragmentation, which is indicative of apoptotic cell death.

### 2.2.6 | Migration assay

The wound-healing assay was employed to assess the impact of the compounds on cell migration. This method is based on measuring cell proliferation in a medium containing the test substance, which indirectly reflects cell migration. Here's an overview of the procedure:

1. A two-compartment silicon well (μ-Dish) with a 500 μm gap between the two chambers was used for this assay.
2. Cells were loaded into each chamber of the two-compartment silicon well at a density of 35,000 cells in 70 μL of medium and incubated for 24 h.
3. After the incubation period, the silicon well was carefully removed using forceps and the old medium was discarded.
4. Approximately 2 mL of fresh medium was added to each chamber and the test compounds were applied at the $GI_{50}$ dose.
5. Starting at this point, photographs were taken at 24 h intervals using the μ-Dish, where the test substances were placed.
6. The photographs were taken until the gap of 500 μm in the μ-Dish, which served as the control, was completely filled.

The wound-healing assay allowed for the observation and quantification of cell migration over time in response to the test compounds.

### 2.2.7 | Esterase method

To evaluate the potential inhibitory effect of methoxyquinoline derivatives on hCA I and II enzymes, we used the esterase activity method for kinetic and inhibitory studies.[44] Spectrophotometric measurement was performed at 348 nm and half-maximal inhibitory concentration ($IC_{50}$) values were calculated using the obtained data. The method is based on the fact that hCA exhibits esterase activity and that the enzyme hCA hydrolyzes p-nitrophenyl acetate, which is used as a substrate, to p-nitrophenol or p-nitrophenolate, which absorbs at 348 nm. The enzyme activity was determined using the following method: Combine the Tris-SO4 (0,5 M) pH 7.4, $H_2O$ and inhibitor solutions in a 1 mL quartz cuvette, adding the substrate (*p*-Nitrophenol acetate) last. The resulting mixture is then measured spectrophotometrically.

The amount of water was adjusted to compensate for the increase in enzyme volume, and the total volume was always brought to 1000 μL. Following the preparation of the reaction mixture, the absorbance at 348 nm at 25°C was measured at the beginning and end of 3 min, and the difference was recorded.

### 2.2.8 | Antibacterial and antifungal activity measurement with microdilution assay

In this study, the antibacterial and antifungal activities of various compounds were assessed using a microdilution assay. The following microbial strains were employed: *Enterococcus faecalis* VRE ATCC 19433, *E. faecalis* ATCC 29212, *Staphylococcus aureus* ATCC 25923, *S. aureus* MSSA ATCC 29213, *S. aureus* MRSA ATCC 46300, *Escherichia coli* ATCC 25922, *Pseudomonas aeruginosa* AGME ATCC

27853, *Streptococcus gordonii* (NCTC 7870), *Aggregatibacter actinomycetemcomitans* (ATCC 33384), and *Candida albicans* (ATCC 10231). To determine the MIC values against bacterial strains, a micro-well dilution method was employed. Bacterial inocula were prepared by using 12 h cultures in Mueller–Hinton broth and the suspensions were adjusted to a 0.5 McFarland standard turbidity. *C. albicans* (ATCC 10231) strain was maintained on solid Sabouraud dextrose agar in an incubator at 35°C. After 24 h, fungal inocula were prepared in RPMI-2% glucose broth, and cell counts were obtained using a Neubauer chamber and trypan blue stain, resulting in a final concentration of $1.5 \times 10^6$ cells/mL. The Trypan blue counting method with a Neubauer chamber was exclusively employed for live *C. albicans* quantification. Each compound was dissolved in DMSO and serial twofold dilutions ranging from 4 to 512 µg/mL were prepared in microplate wells containing nutrient broth. Following a 24 h incubation period at 35°C, microbial growth was assessed visually. The MIC was defined as the lowest concentration at which no visible growth (turbidity) was observed.

## 3 | RESULT AND DISCUSSION

### 3.1 | Chemistry

The aim of this study, as depicted in Scheme 1, was to synthesize polyfunctional aryl tacrine (1,2,3,4-tetrahydroacridine) derivatives through the utilization of brominated tacrines and to investigate their potential anticancer and enzyme inhibition activities. To accomplish this goal, we followed a two-step procedure.

Initially, we synthesized brominated tricyclic tacrine derivatives in accordance with established literature procedures,[21] employing the Friedlander reaction.

Subsequently, we converted the resulting tacrine bromides (**3** and **4**) into the desired diarylated tacrine derivatives using a one-pot Suzuki–Miyaura cross-coupling reaction. In this study, we have detailed the synthesis of diarylated tetrahydroacridine amines (**3a–e** and **4a–e**) through the Suzuki–Miyaura cross-coupling of dibromo tetrahydroacridine amines (**3** and **4**) with various 4-substituted phenylboronic acids (including unsubstituted, 4-ethyl, 4-methoxy, 4-thiomethyl, and 4-trifluoromethoxy derivatives). These reactions were catalyzed by Pd $(PPh_3)_4$ (tetrakis(triphenylphosphine) palladium (0)) and resulted in moderate yields ranging from 51% to 78% (as outlined in Table 1).

The structures of diphenyl arylated tacrines (**3a–e** and **4a–e**) were elucidated through a comprehensive analysis that included $^1$H NMR, $^{13}$C NMR, $^{19}$F NMR, FT-IR spectroscopy, and HRMS. The $^1$H NMR spectra of diphenyl tacrines **3a–e** and **4a–e** exhibited similarities to the starting materials (**3** and **4**), with variations primarily observed in the aromatic phenyl signals and the 4-substituted groups ($-CH_2CH_3$, $-OCH_3$, $-SCH_3$).

In the $^1$H NMR spectra of compounds **3a–e**, the aliphatic triplets (δ 2.92–2.59, δ 2.89–2.55, δ 2.87–2.58, δ 2.92–2.56, and δ 2.88–2.62, respectively) and aliphatic multiplet (δ 1.88, δ 1.30, δ 1.95–1.65, δ 1.90, and δ 1.90–1.65, respectively) correspond to the characteristic Ha'-Hd' protons ($CH_2$) in the six-membered alkyl ring of the tacrines. Similarly, the $^1$H NMR shifts of the Ha-He protons ($CH_2$) of the seven-membered alkyl ring of tacrines **4a–e** also appear as triplets (δ 3.11–2.69, δ 3.16–2.65, δ 3.13–2.71, and δ 3.12–2.72, respectively) and multiplets (δ 1.87–1.72, δ 1.78–1.61, δ 1.80–1.65, δ 1.79–1.64, and δ 1.81–1.62, respectively).

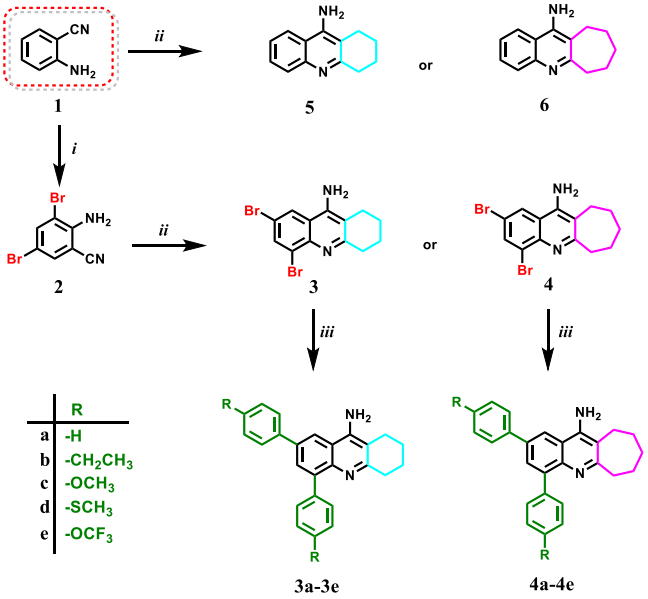


**SCHEME 1** Synthesis of arylated tacrine (**3a–e** and **4a–e**) derivatives. Reagents and conditions: (i) 4.2 eq $Br_2$ in AcOH at 10°C for 5 h (ii). $BF_3.OEt_2$, cyclohexanone (for Compounds **3** and **5**) or cycloheptanone (for Compounds **4** and **6**) in toluen. 2 M NaOH(aq) at reflux for 24 h (iii) arylboronic acid, $Pd(PPh_3)_4$, 3 M $K_2CO_3$(aq) in 1,4-dioxane at reflux for 5 h.

**TABLE 1** Yields and melting points of synthesized diarylated tacrine derivatives (**3a–e** and **4a–e**).

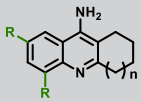

| Boronic acid | Solvent | Product | *n* | Yield (%) | M.p. (°C) |
|---|---|---|---|---|---|
|  | 1,4-Dioxane | **3a** | 1 | 51 | 209–210 |
| | | **4a** | 2 | 60 | 134–135 |
|  | 1,4-Dioxane | **3b** | 1 | 63 | 182–183 |
| | | **4b** | 2 | 61 | 105–108 |
| 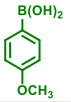 | 1,4-Dioxane | **3c** | 1 | 58 | 170–171 |
| | | **4c** | 2 | 55 | 125–128 |
| 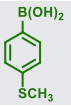 | 1,4-Dioxane | **3d** | 1 | 63 | 131–132 |
| | | **4d** | 2 | 78 | 184–186 |
| 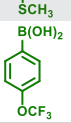 | 1,4-Dioxane | **3e** | 1 | 67 | 131–132 |
| | | **4e** | 2 | 62 | 100–102 |

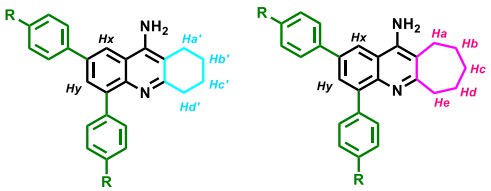


**FIGURE 1** General representation of the aliphatic protons of the diarylated tacrine synthesized (**3a–e** and **4a–e**).

The Hx protons of **3a–e** gave singlets at 7.94, 8.12, 7.81, 7.95, 7.85 ppm, respectively, while the Hy protons of **3a–e**, apart from **3a** and **3b** ($\delta$ 7.85), were not distinctly discernible as singlet signals, often overlapping with other signals. In the case of **4a–e**, the Hx and Hy protons (Figure 1) did not appear as clear singlets but were observed adjacent to or overlapping each other. It is noteworthy that the synthesized tacrines are structurally asymmetric molecules.

Unexpectedly, the $^{1}$H NMR signals of the aromatic diphenyl protons (doublet) of **3c** and **3e** displayed symmetrical properties, which was an intriguing observation. On the other hand, all aromatic phenyl protons of other tacrines displayed mixed signals as doublets or multiplets.

The $^{1}$H NMR spectra of **3b** and **4b**, featuring overlapping triplets and quartets at approximately 2.73 and 1.30 ppm, respectively, confirmed the attachment of two (4-ethyl)phenyl groups instead of Br atoms to the tacrine rings. Moreover, the two singlets in the **3c** and **4c** spectra at nearly 3.80 ppm, corresponding to the -$OCH_3$ protons, provided supporting evidence for the linkage of 4-(methoxy) phenyl groups to the tacrine ring. The -$SCH_3$ protons (**3d** and **4d**) of the bonded 4-(methylthio)phenyl group were confirmed by two singlets each, appearing around 2.50 ppm.

In the $^{19}$F NMR spectra of **3e** and **4e**, two singlets at −58.0 and −58.2 ppm provided clear evidence for the presence of the 4-(trifluoromethoxy)phenyl group in the tacrine.

In the $^{13}$C NMR spectra of compounds **3a–e** and **4a–e**, the presence of four (for **3a–e**) and five (for **4a–e**) aliphatic carbon resonances (~23.0–40.0 ppm) in the $sp^3$ hybridization and 21 aromatic carbon resonances further supported the structural identities of these compounds.

## 3.2 | Anticancer activities

Numerous studies in the literature have reported the diverse bioactivities of quinoline derivatives, with a particular emphasis on their potential anticancer properties. Although the AChE inhibition properties of tacrine derivatives, which consist of six-membered or seven-membered aliphatic rings fused to the quinoline skeleton, are well-established, investigations into their anticancer potential have been relatively limited. The initial studies on this subject were conducted by our research group.[7,8]

### 3.2.1 | Evaluation of new molecules according to NCI60 screening methodology

Anticancer properties of tacrine derivatives have been explored in only a limited number of studies within literature. In our recent research,[8] we have made significant advancements by reporting noteworthy antiproliferative effects of tacrine derivatives, specifically those incorporating tricyclic quinoline structures, against HT29 cell lines using the MTT assay.

In our ongoing efforts to address both primary and acquired chemotherapeutic resistance mechanisms and mitigate drug-related side effects, our research group is committed to developing novel and effective therapeutic agents for cancer treatment. In this regard, we have conducted MTT tests to assess the impact of newly synthesized diarylated tacrine analogs, created by our research team, on cell proliferation. These tests were conducted following the NCI-60 screening methodology.

Upon comparing the novel tacrine analogs (**3a–e** and **4a–e**) with the starting compounds (dibrominated tacrines) **3** and **4**, as well as nonsubstituted tacrines **5** and **6**, we observed their potent anticancer effects against A549 and Calu1 lung cancer cell lines, with $GI_{50}$ values ranging from 1.01 to 1.94 μg/mL and TGI values from 1.06 to 17.9 μg/mL (Table 2). Similar results were obtained when evaluating the anticancer effects of these compounds on MCF7 breast cancer cells, with $GI_{50}$ values ranging from 1.02 to 1.65 μg/mL and TGI values from 1.21 to 3.85 μg/mL (Table 2).

These diarylated tacrine derivatives **3a–e** and **4a–e** exhibited better antiproliferative activity compared to the control drug, 5-Fluorouracil (5-FU), in HeLa, A2780, and A2780ADR gynecologic cancer cell lines, with $GI_{50}$ values in the range of 1.02–1.54 μg/mL and TGI values from 1.22 to 5.13 μg/mL (Table 3). Furthermore, the tested novel tacrine compounds (**3a–e** and **4–e**) demonstrated superior inhibition of cell proliferation compared to the control drug, 5-FU, in SW620 and HT29 colon cancer cell lines, with $GI_{50}$ values ranging from 1.02 to 1.78 μg/mL and TGI values from 1.01 to 4.87 μg/mL (Table 3).

In addition, we evaluated the antiproliferative effects of these novel molecules **3a–e** and **4a–e** against Saos2, MG63, and SW1353 bone cancer cell lines, and found that they exhibited strong antiproliferative effects, with $GI_{50}$ values ranging from 1.01 to 1.87 μg/mL and TGI values from 1.12 to 7.04 μg/mL (Table 4).

On the other hand, when assessing the antiproliferative effects of these diarylated tacrines **3a-e** and **4a-e** on normal cell lines (Beas2B, FL, and HC cells), we found that these compounds demonstrated safety, with $GI_{50}$ values ranging from 1.01 to 1.93 μg/mL and TGI values from 1.03 to 3.28 μg/mL (Tables 2 and 4). However, upon careful examination of Tables 2–4, it is evident that the antiproliferative activity of diarylated substituted tacrines remained at a lower level than the control anticancer drug, 5-FU, in normal cells, while they exhibited a stronger anticancer effect on cancer cells (Tables 2 and 4).

The introduction of a bromine atom to the six-membered tacrine (**5**, TGI = 19.6 μg/mL) compound at positions C-6 and C-8

**TABLE 2** $GI_{50}$,[a] TGI,[a] and $LC_{50}$[a] values for tested compounds against cancer cell lines A549, Calu1, HeLa, A2780, and A2780ADR.

| | A549 (μg/mL)[b] | | | Calu1 (μg/mL)[b] | | | HeLa (μg/mL)[b] | | | A2780 (μg/mL)[b] | | | A2780ADR (μg/mL)[b] | | |
|---|---|---|---|---|---|---|---|---|---|---|---|---|---|---|---|
| **Comp#** | **$GI_{50}$** | **TGI** | **$LC_{50}$** | **$GI_{50}$** | **TGI** | **$LC_{50}$** | **$GI_{50}$** | **TGI** | **$LC_{50}$** | **$GI_{50}$** | **TGI** | **$LC_{50}$** | **$GI_{50}$** | **TGI** | **$LC_{50}$** |
| **3a** | 1.12 | 1.64 | 7.14 | 1.03 | 1.06 | 2.99 | 1.47 | 2.71 | 18.3 ± 0.9 | 1.32 | 2.40 | 15.7± | 1.25 | 2.59 | 55.7 ± 2.8 |
| **3b** | 1.01 | 1.11 | 2.38 | 1.03 | 1.09 | 1.13 | 1.21 | 2.06 | 14.5 ± 0.6 | 1.02 | 1.22 | 4.51 | 1.36 | 3.27 | 95.3 ± 3.9 |
| **3c** | 1.12 | 1.57 | 6.17 | 1.02 | 1.08 | 3.63 | 1.13 | 1.82 | 18.7 ± 0.9 | 1.18 | 1.81 | 8.21 | 1.18 | 2.18 | 34.3 ± 1.7 |
| **3d** | 1.19 | 1.79 | 6.91 | 1.09 | 1.69 | 12.2 ± 0.7 | 1.19 | 2.08 | 20.1 ± 1.0 | 1.15 | 1.88 | 16.0 ± 0.9 | 1.13 | 1.74 | 9.24 |
| **3e** | 1.31 | 2.63 | 30.4 ± 1.3 | 1.39 | 2.71 | 20.1 ± 1.0 | 1.26 | 2.56 | 41.7 ± 2.0 | 1.24 | 2.17 | 15.7 ± 0.8 | 1.26 | 2.43 | 25.2 ± 1.0 |
| **4a** | 1.19 | 1.93 | 10.2 ± 0.6 | 1.17 | 1.62 | 11.3 ± 0.7 | 1.25 | 2.51 | 44.9 ± 1.9 | 1.04 | 1.32 | 5.76 | 1.11 | 1.77 | 21.4 ± 1.0 |
| **4b** | 1.19 | 2.23 | 31.9 ± 1.2 | 1.21 | 1.97 | 12.7 ± 0.8 | 1.26 | 2.59 | 36.4 ± 1.7 | 1.14 | 1.72 | 9.24 | 1.26 | 2.32 | 21.9 ± 1.0 |
| **4c** | 1.21 | 1.93 | 9.54 | 1.01 | 1.14 | 4.08 | 1.21 | 2.13 | 19.6 ± 0.8 | 1.24 | 1.96 | 8.28 | 1.27 | 2.59 | 42.1 ± 2.1 |
| **4d** | 1.25 | 16.5 ± 0.7 | >500 | 1.27 | 5.62 | >500 | 1.21 | 2.29 | 36.2 ± 1.4 | 1.12 | 1.77 | 16.1 ± 0.8 | 1.04 | 1.37 | 8.48 |
| **4e** | 1.94 | 17.9 ± 0.7 | >500 | 1.52 | 4.23 | 138.9 ± 2.2 | 1.44 | 3.24 | 43.7 ± 1.8 | 1.44 | 2.91 | 22.4 ± 1.0 | 1.54 | 5.13 | 448.7 ± 18 |
| **3** | 2.94 | 80.6 ± 3.1 | >500 | 1.42 | 4.43 | >500 | 1.32 | 3.5 | 331.6 ± 16 | 1.95 | 7.93 | >500 | 1.39 | 5.27 | >500 |
| **4** | 2.61 | 31.2 ± 1.6 | >500 | 1.64 | 5.75 | 459.3 ± 17 | 2.25 | 15.7 ± 0.8 | >500 | 1.94 | 11.8 ± 0.7 | >500 | 1.55 | 9.91 | >500 |
| **5** | 2.31 | 19.6 ± 1.0 | >500 | 1.94 | 7.22 | 351.4 ± 15 | 1.78 | 7.85 | >500 | 2.19 | 9.88 | >500 | 1.36 | 5.05 | >500 |
| **6** | 2.78 | 104.5 ± 6.3 | >500 | 1.95 | 15.1 ± 0.7 | >500 | 1.38 | 4.29 | >500 | 1.17 | 2.54 | 214.5 ± 8.1 | 1.54 | 5.21 | >500 |
| **5-FU** | 1.44 | 47.1 ± 1.7 | 470.0 ± 18 | 1.72 | 61.8 ± 3.1 | 450.4 ± 16 | 1.78 | 39.7 ± 1.4 | 439.0 ± 19 | 1.43 | 51.7 ± 2.3 | 423.8 ± 17 | 1.55 | 50.9 ± 3.7 | 441.6 ± 20 |

Abbreviations: 5-FU, 5-Fluorouracil; TGI, total growth inhibition.

[a]Percent inhibition noted is mean values ± SDs of three independent measures.

[b]If percent inhibition is <10, the SD value is <0.5.

**TABLE 3** $GI_{50}$,[a] TGI,[a] and $LC_{50}$[a] values for tested compounds against cancer cell lines Saos2, MG63, SW1353, HT29, and SW620.

| | Saos2 (μg/mL)[b] | | | MG63 (μg/mL)[b] | | | SW1353 (μg/mL)[b] | | | HT29 (μg/mL)[b] | | | SW620 (μg/mL)[b] | | |
|---|---|---|---|---|---|---|---|---|---|---|---|---|---|---|---|
| **Comp #** | **$GI_{50}$** | **TGI** | **$LC_{50}$** | **$GI_{50}$** | **TGI** | **$LC_{50}$** | **$GI_{50}$** | **TGI** | **$LC_{50}$** | **$GI_{50}$** | **TGI** | **$LC_{50}$** | **$GI_{50}$** | **TGI** | **$LC_{50}$** |
| **3a** | 1.28 | 2.71 | 51.6 ± 2.9 | 1.26 | 3.82 | 2.8 ± 1.9 | 1.01 | 1.12 | 3.16 | 1.24 | 2.01 | 9.42 | 1.03 | 1.21 | 2.73 |
| **3b** | 1.12 | 1.81 | 21.7 ± 1.5 | 1.19 | 2.19 | 19.7 ± 0.9 | 1.17 | 1.86 | 10.2 ± 0.6 | 1.02 | 1.18 | 3.56 | 1.16 | 1.01 | 1.14 |
| **3c** | 1.16 | 2.09 | 36.4 ± 1.8 | 1.38 | 4.12 | 33.3 ± 1.2 | 1.01 | 1.14 | 3.65 | 1.14 | 1.61 | 5.49 | 1.02 | 1.15 | 2.59 |
| **3d** | 1.27 | 2.61 | 42.7 ± 2.0 | 1.11 | 2.43 | 37.2 ± 1.9 | 1.06 | 1.53 | 16.7 ± 0.9 | 1.39 | 2.42 | 10.6 ± 0.6 | 1.05 | 1.28 | 3.11 |
| **3e** | 1.38 | 3.15 | 57.7 ± 2.2 | 1.35 | 4.17 | 43.1 ± 2.0 | 1.24 | 2.21 | 17.2 ± 0.8 | 1.34 | 2.34 | 11.9 ± 0.6 | 1.54 | 2.85 | 12.7 ± 0.6 |
| **4a** | 1.22 | 2.46 | 53.5 ± 2.9 | 1.21 | 3.24 | 48.8 ± 2.1 | 1.11 | 1.60 | 7.67 | 1.04 | 1.28 | 3.82 | 1.16 | 1.72 | 6.12 |
| **4b** | 1.29 | 2.85 | 72.1 ± 3.1 | 1.14 | 3.74 | 53.2 ± 2.1 | 1.15 | 1.65 | 12.1 ± 0.6 | 1.05 | 1.31 | 4.76 | 1.36 | 1.23 | 3.54 |
| **4c** | 1.19 | 2.17 | 24.6 ± 1.4 | 1.41 | 3.17 | 28.4 ± 1.1 | 1.11 | 1.87 | 40.2 ± 2.0 | 1.25 | 2.05 | 8.13 | 1.17 | 1.63 | 4.52 |
| **4d** | 1.47 | 3.93 | 125.2 ± 4.1 | 1.32 | 3.62 | 118.7 ± 4.0 | 1.19 | 2.04 | 17.6 ± 0.9 | 1.22 | 1.95 | 9.39 | 1.44 | 2.49 | 11.0 ± 0.6 |
| **4e** | 1.86 | 7.04 | 449.8 ± 18 | 1.77 | 5.92 | 372.4 ± 11 | 1.87 | 5.64 | 116.6 ± 4.1 | 1.22 | 2.48 | 42.2 ± 2.0 | 1.78 | 4.87 | 71.3 ± 2.3 |
| **3** | 1.55 | 6.53 | >500 | 1.63 | 9.34 | >500 | 2.16 | 15.2 ± 0.7 | >500 | 1.26 | 5.18 | >500 | 2.54 | 17.7 ± 1.0 | >500 |
| **4** | 1.97 | 9.35 | >500 | 1.81 | 1.9 ± 0.6 | >500 | 2.61 | 26.8 ± 1.1 | >500 | 1.44 | 4.33 | 326.5 ± 15 | 2.61 | 24.1 ± 1.1 | >500 |
| **5** | 2.12 | 12.6 ± 0.7 | >500 | 2.03 | 3.1 ± 0.6 | >500 | 1.47 | 3.64 | 74.8 ± 2.8 | 1.37 | 4.32 | >500 | 2.21 | 11.0 ± 0.7 | >500 |
| **6** | 1.94 | 15.4 ± 0.9 | >500 | 1.78 | 2.7 ± 0.6 | >500 | 2.31 | 14.9 ± 0.8 | >500 | 2.44 | 26.1 ± 1.1 | >500 | 2.56 | 36.4 ± 1.3 | >500 |
| **5-FU** | 1.43 | 42.7 ± 2.0 | 431.2 ± 19 | 1.82 | 52.7 ± 2.8 | 429.4 ± 21 | 1.56 | 40.5 ± 1.9 | 409.3 ± 15 | 1.66 | 39.0 ± 1.7 | 453.8 ± 19 | 1.52 | 34.9 ± 1.9 | 399.8 ± 18 |

Abbreviations: 5-FU, 5-Fluorouracil; TGI, total growth inhibition.

[a]Percent inhibition noted is mean values ± SDs of three independent measures.

[b]If percent inhibition is <10, the SD value is <0.5.

**TABLE 4** $GI_{50}$,[a] TGI,[a] and $LC_{50}$[a] values for tested compounds against cancer cell line MCF7 and healthy cell lines Beas2B, FL and HC.

| | MCF7 (μg/mL)[b] | | | Beas2B[c] (μg/mL)[b] | | | FL[c] (μg/mL)[b] | | | HC[c] (μg/mL)[b] | | |
|---|---|---|---|---|---|---|---|---|---|---|---|---|
| Comp # | $GI_{50}$ | TGI | $LC_{50}$ | $GI_{50}$ | TGI | $LC_{50}$ | $GI_{50}$ | TGI | $LC_{50}$ | $GI_{50}$ | TGI | $LC_{50}$ |
| **3a** | 1.16 | 1.81 | 10.2 ± 0.6 | 1.24 | 2.08 | 12.0 ± 0.8 | 1.05 | 1.05 | 1.85 | 1.04 | 1.27 | 3.58 |
| **3b** | 1.02 | 1.21 | 4.37 | 1.27 | 1.94 | 10.6 ± 0.6 | 1.04 | 1.35 | 7.32 | 1.09 | 1.12 | 1.24 |
| **3c** | 1.04 | 1.28 | 3.94 | 1.25 | 2.18 | 28.8 ± 1.4 | 1.01 | 1.04 | 1.89 | 1.03 | 1.25 | 3.58 |
| **3d** | 1.06 | 1.38 | 5.77 | 1.16 | 1.95 | 18.8 ± 1.6 | 1.05 | 1.33 | 4.36 | 1.09 | 1.49 | 3.94 |
| **3e** | 1.27 | 2.11 | 10.2 ± 0.6 | 1.38 | 2.69 | 20.0 ± 1.8 | 1.21 | 1.78 | 5.63 | 1.15 | 1.86 | 15.5 ± 0.8 |
| **4a** | 1.12 | 1.66 | 8.86 | 1.21 | 2.06 | 15.9 ± 1.5 | 1.06 | 1.33 | 3.59 | 1.20 | 1.97 | 11.8 ± 0.6 |
| **4b** | 1.03 | 1.26 | 4.45 | 1.28 | 2.46 | 24.4 ± 1.8 | 1.03 | 1.19 | 2.97 | 1.05 | 1.34 | 5.32 |
| **4c** | 1.03 | 1.28 | 5.15 | 1.16 | 1.92 | 16.9 ± 1.0 | 1.06 | 1.03 | 1.79 | 1.03 | 1.23 | 3.59 |
| **4d** | 1.08 | 1.49 | 7.66 | 1.12 | 1.82 | 22.2 ± 1.9 | 1.28 | 2.06 | 8.28 | 1.93 | 3.28 | >500 |
| **4e** | 1.65 | 3.85 | 36.6 ± 2.0 | 1.45 | 3.19 | 36.1 ± 2.1 | 1.47 | 3.07 | 26.3 ± 1.3 | 1.24 | 2.94 | 222.7 ± 7.1 |
| **3** | 2.04 | 9.13 | >500 | 1.38 | 3.19 | 153.8 ± 6.3 | 1.92 | 5.68 | 98.1 ± 3.8 | 1.65 | 8.63 | >500 |
| **4** | 1.04 | 1.56 | 36.8 ± 1.4 | 1.27 | 9.47 | >500 | 2.02 | 7.16 | 246.5 ± 5.1 | 2.28 | 22.3 ± 1.0 | >500 |
| **5** | 1.54 | 3.91 | 72.0 ± 3.7 | 1.63 | 5.49 | 381.7 ± 12 | 1.81 | 5.17 | 92.9 ± 3.0 | 1.11 | 2.01 | 78.7 ± 2.9 |
| **6** | 2.03 | 8.33 | >500 | 1.75 | 7.51 | >500 | 2.05 | 8.32 | >500 | 1.28 | 3.59 | >500 |
| **5-FU** | 1.86 | 70.6 ± 3.1 | 480.1 ± 19 | 1.50 | 52.7 ± 2.0 | 428.9 ± 17 | 1.43 | 41.2 ± 2.1 | 407.5 ± 18 | 1.66 | 57.2 ± 2.3 | 433.6 ± 18 |

Abbreviations: 5-FU, 5-Fluorouracil; TGI, total growth inhibition.

[a]Percent inhibition noted is mean values ± SDs of three independent measures.

[b]If percent inhibition is <10, the SD value is <0.5.

[c]Beas2B, FL, and HC are healthy cell lines. Their inhibition values are colored as green for the new compounds (**3a–e**, **4a–e**), yellow for the starting materials (**3**–**6**), and blue for the control compound (5-FU).

significantly decreased its antiproliferative activity against A549 cancer cell lines (**3**, TGI = 80.6 μg/mL). Conversely, adding a bromine atom to the seven-membered tacrine structure (**4**) at position 6 (TGI = 104.5 μg/mL) resulted in a substantial inhibition of proliferation, with a TGI of 31.2 μg/mL. However, it's important to note that these effects were primarily observed in the A549 cell line, and no significant differences were noted in other cell lines.

Across all cancer cell lines, Compounds **3**–**6** displayed lower antiproliferative activity at lower concentrations compared to the control compound (5-FU). This indicates that, although the bromine substitutions had varied effects on the A549 cell line, the overall antiproliferative activity of these compounds was generally more potent than that of 5-FU when tested against the studied cancer cell lines.

Additionally, Compounds **3a**–**e** and **4a**–**e**, which were derived from the key Compounds **3** and **4**, exhibited a more pronounced ability to inhibit the proliferation of cancer cells in comparison to their starting compounds (**3** and **4**) and the unsubstituted tacrines (**5** and **6**). This enhanced antiproliferative activity was particularly noteworthy against a wide range of cancer cell lines, including MCF7, HeLa, A2780, A2780ADR, SW620, HT29, A549, Calu1, Saos2, MG63, and SW1353. These findings suggest that the novel derivatives, **3a**–**e** and **4a**–**e**, possess promising potential as antiproliferative agents against various cancer cell types.

In the NCI60 screening methodology, high $LC_{50}$ values, indicating less cytotoxic effects, are desirable. Simultaneously, low $GI_{50}$ and TGI values, which represent a strong cytostatic effect, are also preferable features. When we compare the novel tacrines to 5-FU in terms of $GI_{50}$ and TGI values, it is evident that these molecules fall within the safe usage limits for all cell lines (Tables 2–4). Generally, if the anticancer effects of molecules are weak, their $LC_{50}$ values tend to be higher.

Examining the effects of these molecules, particularly in lung, gynecologic, bone, and colon cancer cell lines, where they stand out in terms of NCI60 survival parameters, it's evident that their $GI_{50}$, TGI, and $LC_{50}$ values fall within the desired range. These results strongly suggest that these molecules exhibit cancer-specific activity for these specific types of cancer.

Notably, when considering all treated cancer cell lines, two novel compounds, 2,4-Bis(4-(trifluoromethoxy)phenyl)−7,8,9,10-tetrahydro-6H-cyclohepta[b]quinolin-11-amine (**4e**) ($LC_{50}$ values 22.4–>500 μg/mL for cancer cells and 26.3–222.7 μg/mL for normal cells), 2,4-bis(4-(methylthio)phenyl)−7,8,9,10-tetrahydro-6H-cyclohepta[b]quinolin-11-amine (**4d**) ($LC_{50}$ values 7.6–>500 μg/mL for cancer cells and 8.3–>500 μg/mL for normal cells), and two starting molecules, 5,7-dibromo-1,2,3,4-tetrahydroacridine-9-amine (**3**) ($LC_{50}$ values 331.6–>500 μg/mL for cancer cells and 98.1–>500 μg/mL for normal cells) and 2,4-dibromo-7,8,9,10-tetrahdro-6H-cyclohepta[b]quinolin-11-amine (**4**) ($LC_{50}$ values 36.8–>500 μg/mL for cancer cells and

246.5–>500 μg/mL for normal cells) are the most promising compounds for further preclinical studies. These findings suggest that these compounds have the potential for effective cancer-specific treatments and deserve further investigation.

### 3.2.2 | Cytotoxic activity of the new molecules

The assessment of cytoplasmic LDH enzyme release into the extracellular environment due to membrane disruptions caused by novel tacrine derivatives (**3a–e** and **4a–e**) offers insights into their cytotoxic activities. Cytoplasmic LDH activity was quantified using an LDH cytotoxicity kit in this study. Cytotoxicity induced by the novel tacrine derivatives (**3a–e** and **4a–e**) was measured at TGI concentrations.

Consequently, these compounds (**3a–e** and **4a–e**), which demonstrated effectiveness in the MTT proliferation test, exhibited acceptably low cytotoxicity values, ranging from ~7.3% to 27.9%, for Beas2B, FL, and HC normal cell lines at TGI concentration (Table 5). The cytotoxic effects of the tested novel tacrine derivatives (**3a–e** and **4a–e**) were found to be effective in the MTT proliferation assay, with LDH % values in the range of 8.7% to 29.7% for lung cancer cells (A549 and Calu1), 11.4% to 27.0% for gynecologic cancer cells (HeLa, A2780, and A2780ADR), 9.2% to 23.1% for bone cancer cells (Saos2, MG63, and SW1353), 9.4% to 28.6% for colon cancer cells (SW620 and HT29), and 15.1% to 27.7% for breast cancer cells (MCF7) at TGI concentration, respectively (Table 5).

Based on these results, the cytoplasmic LDH activity measurements of novel tacrine derivatives revealed that, particularly, novel compound **4e** (LDH % values ranging between 7.3% and 18.5%) and the starting Compounds **3**–**6** (LDH % values ranging between 9.29% and 21.6%) induced the lowest level of membrane damage at their TGI concentration for all tested cell lines (Table 5), when compared to both the control (5-FU, LDH % values ranging between 13.4% and 16.7%) and all the other newly synthesized molecules (**3a**–**4d**). It has been observed that these compounds exert a cytostatic effect. Consequently, when considering the results from both the MTT assay (which indicates therapeutic potential) and the LDH assay (indicating cytotoxicity), it is evident that Compound **4e** exhibits the most optimal antiproliferative and cytotoxic effects against both cancer and normal cells, surpassing the positive control, 5-FU (Tables 2–5).

In summary, the tested novel compounds (**3a–e** and **4a–e**) demonstrate acceptable toxicity towards cancer cell lines while maintaining safety for normal cells, providing a promising basis for further preclinical studies.

### 3.2.3 | Evaluation of mitochondrial membrane potential

The mitochondrial membrane potential of the novel arylated tacrine **3d** and its starting material **3** was assessed by staining with Rhodamine 123. Intense green fluorescence is indicative of cells with a high mitochondrial

**TABLE 5** % Cytotoxicity for tested compounds at TGI concentrations against the cells.[a,b]

| Comp # | A549 | Calu1 | HeLa | A2780 | A2780ADR | Saos2 | MG63 | SW1353 | HT29 | SW620 | MCF7 | FL[c] | HC[c] | Beas2B[c] |
|---|---|---|---|---|---|---|---|---|---|---|---|---|---|---|
| **3a** | 26.8 | 29.6 | 16.0 | 23.0 | 15.4 | 16.5 | 15.0 | 21.7 | 17.6 | 28.6 | 26.8 | 26.2 | 25.4 | 17.5 |
| **3b** | 28.6 | 29.7 | 15.4 | 26.8 | 15.1 | 22.6 | 18.1 | 23.1 | 26.8 | 28.1 | 27.7 | 26.8 | 24.9 | 24.7 |
| **3c** | 25.9 | 29.1 | 16.5 | 25.9 | 16.0 | 16.9 | 12.7 | 22.4 | 25.1 | 28.3 | 26.4 | 27.4 | 24.6 | 18.2 |
| **3d** | 28.1 | 24.7 | 14.3 | 24.5 | 25.6 | 15.9 | 14.4 | 16.1 | 15.2 | 23.9 | 26.7 | 25.2 | 22.1 | 25.0 |
| **3e** | 26.4 | 24.0 | 13.7 | 26.2 | 20.8 | 19.3 | 11.8 | 15.2 | 19.3 | 16.4 | 19.5 | 26.0 | 23.4 | 21.7 |
| **4a** | 25.3 | 25.6 | 15.1 | 24.2 | 25.8 | 16.8 | 13.5 | 17.4 | 25.3 | 24.7 | 26.1 | 25.9 | 21.7 | 22.1 |
| **4b** | 27.1 | 29.5 | 14.9 | 27.0 | 16.6 | 17.7 | 12.3 | 19.0 | 26.7 | 27.4 | 25.6 | 25.8 | 24.8 | 18.3 |
| **4c** | 29.1 | 28.4 | 15.6 | 26.3 | 15.9 | 18.2 | 15.6 | 22.9 | 18.4 | 27.5 | 27.0 | 27.9 | 25.0 | 25.8 |
| **4d** | 8.7 | 23.8 | 12.9 | 25.8 | 27.5 | 14.9 | 12.1 | 15.8 | 22.6 | 17.5 | 27.4 | 24.6 | 18.9 | 24.4 |
| **4e** | 9.5 | 14.2 | 15.8 | 16.1 | 17.1 | 12.5 | 10.6 | 12.6 | 18.5 | 14.2 | 14.8 | 9.7 | 7.3 | 12.9 |
| **3** | 12.4 | 20.3 | 15.5 | 17.0 | 14.9 | 11.9 | 14.1 | 10.8 | 11.4 | 12.3 | 12.9 | 14.0 | 13.3 | 16.9 |
| **4** | 10.8 | 19.8 | 11.4 | 12.6 | 13.1 | 12.1 | 10.8 | 9.2 | 15.8 | 10.1 | 21.6 | 14.8 | 9.5 | 15.3 |
| **5** | 11.2 | 18.1 | 12.9 | 12.1 | 13.7 | 13.2 | 11.3 | 10.5 | 14.3 | 10.0 | 17.0 | 15.1 | 16.0 | 15.7 |
| **6** | 9.3 | 14.6 | 16.2 | 19.2 | 14.2 | 10.4 | 14.5 | 15.2 | 9.3 | 9.4 | 15.1 | 13.6 | 14.7 | 14.2 |
| **5-FU** | 14.8 | 16.7 | 16.1 | 14.3 | 15.8 | 15.8 | 14.7 | 13.4 | 16.0 | 14.9 | 13.8 | 15.7 | 15.1 | 15.0 |

Abbreviations: 5-FU, 5-Fluorouracil; TGI, total growth inhibition.

[a]Percent cytotoxicity was noted as mean values ± SDs of three independent measures.

[b]Percent inhibition is <2.0.

[c]Beas2B, FL and HC are healthy cell lines. Their cytotoxicity values are colored as green for the new compounds (3a-e, 4a-e), yellow for the starting materials (3-6) and blue for the control compound (5-FU).

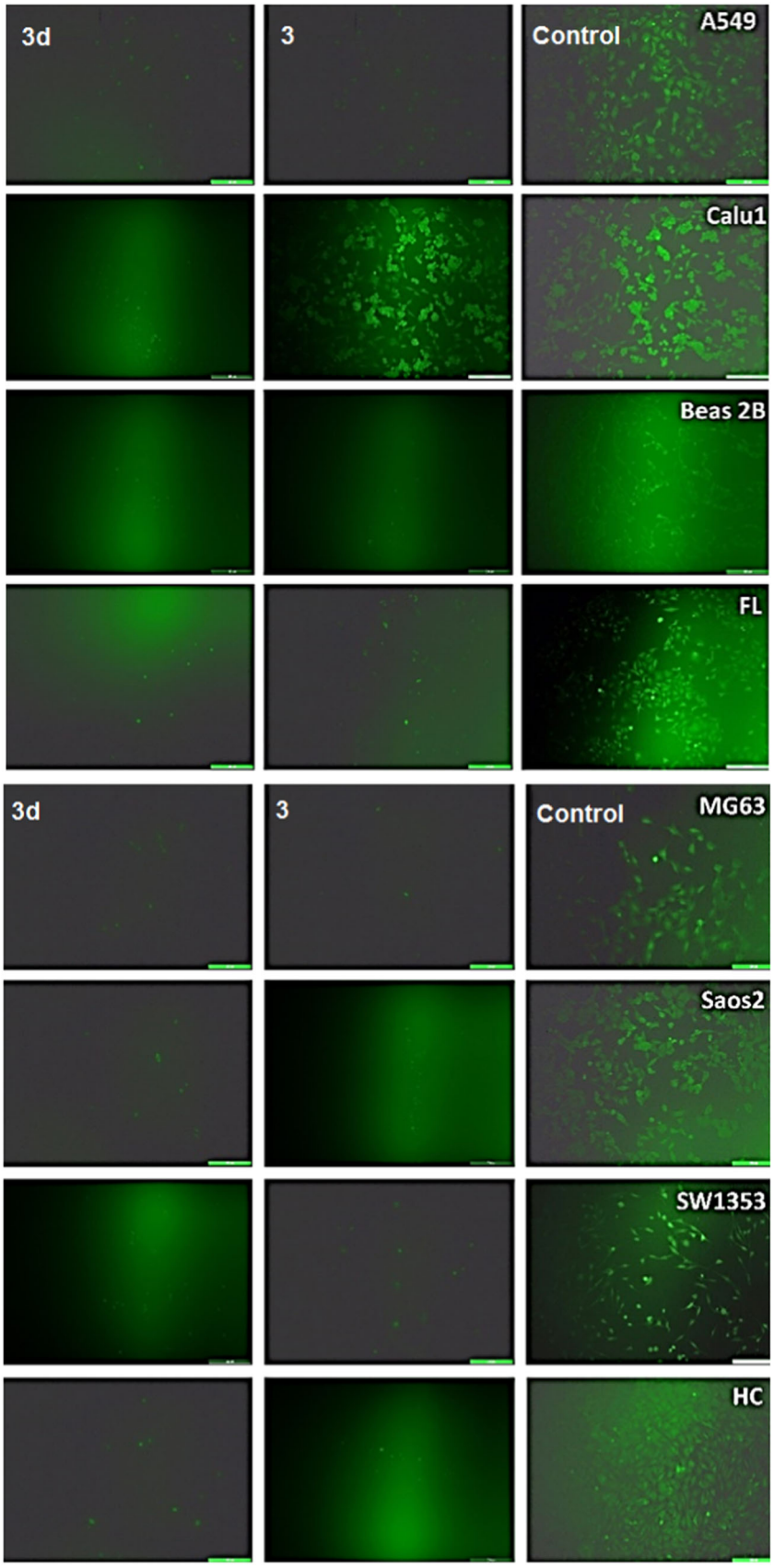


**FIGURE 2** Mitochondrial staining using Rhodamine 123 of the cancer cells in the presence or absence of the **3d** and **3**. All scales are 100 μm.

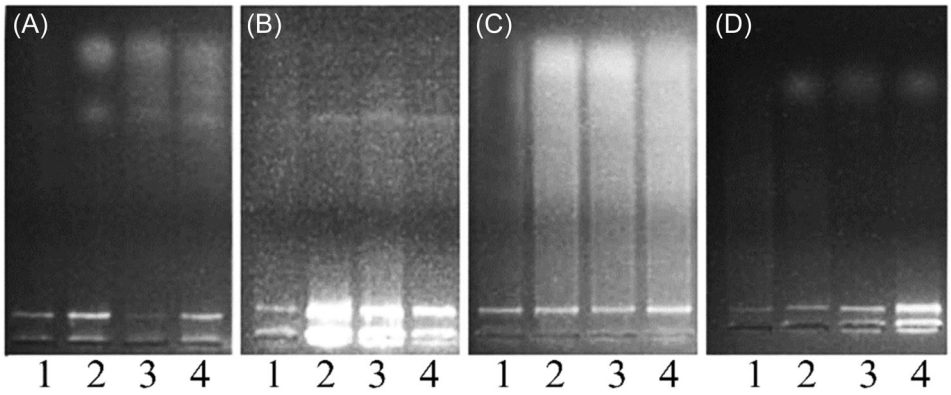


**FIGURE 3** Effects of **3d** (2), **4e** (3), and **3a** (4) molecules on DNA laddering in MG63 (A), HC (B), A549 (C), and Beas2B (D) cell lines. Well (1) is untreated control for all cells.

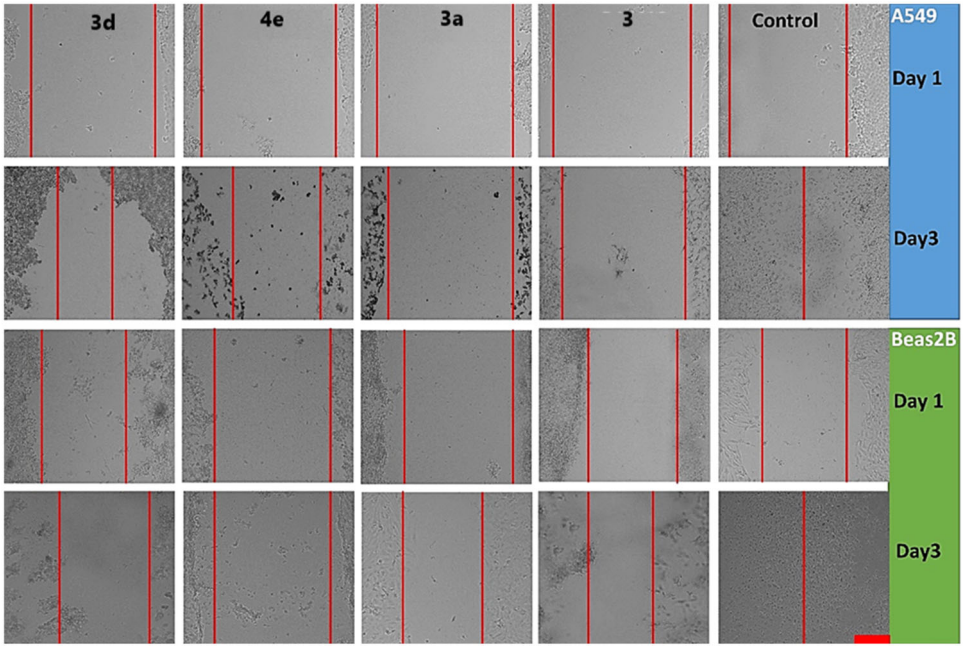


**FIGURE 4** Effects of **3d**, **4e**, **3a** and **3** on cell migration on A549 and Beas2B cell lines. All scales are 100 µm.

membrane potential, suggesting viability. In Figure 2, it is evident that the mitochondrial membrane potential decreased in all cells treated with Compounds **3** and **3d**, as evidenced by the reduced fluorescence compared to untreated cells. The fluorescence intensity in the treatment group was noticeably lower than in the untreated group. The disruption of mitochondrial membrane potential can initiate mitochondria-mediated apoptosis. These findings suggest that the disturbance of mitochondrial membrane potential in cells plays a partial role in the anticancer effects of the novel tacrine derivatives.

### 3.2.4 | DNA degradation

In the apoptotic process, a specific caspase-activated DNase leads to the targeted cleavage of DNA at internucleosomal linker sites, resulting in characteristic fragments of ~200 base pairs that appear as a ladder-like pattern. Thus, apoptotic DNA exhibits a ladder-like appearance when analyzed on an agarose gel. Utilizing the agarose gel DNA laddering method to detect DNA fragments is instrumental in assessing the apoptotic status in a cell. The results of the DNA laddering test revealed that compounds **3d** (Well 2), **4e** (Well 3), and **3a** (Well 4) induced the formation of DNA fragments in treated MG63, HC, A549, and Beas2B cells compared to untreated cells (Figure 3). It is worth noting that there was less DNA fragmentation in the control cells (HC [B] and Beas2B [D]) compared to the cancer cells (MG63 [A] and A549 [C]). This suggests that the test substances do not trigger the apoptotic mechanism as much in normal cells and are therefore less toxic to these cells. This observation underscores that the novel arylated tacrine derivatives exhibit stronger anticancer effects on cancer cells than on normal cells. In the untreated cells

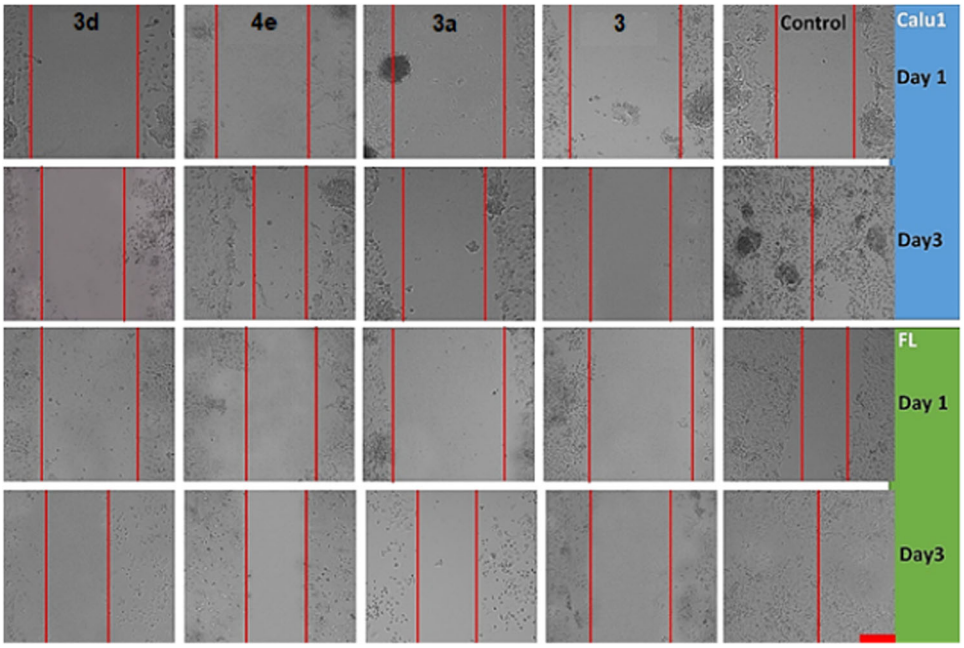


**FIGURE 5** Effects of **3d**, **4e**, **3a**, and **3** on cell migration on Calu1 and FL cell lines. All scales are 100 µm.

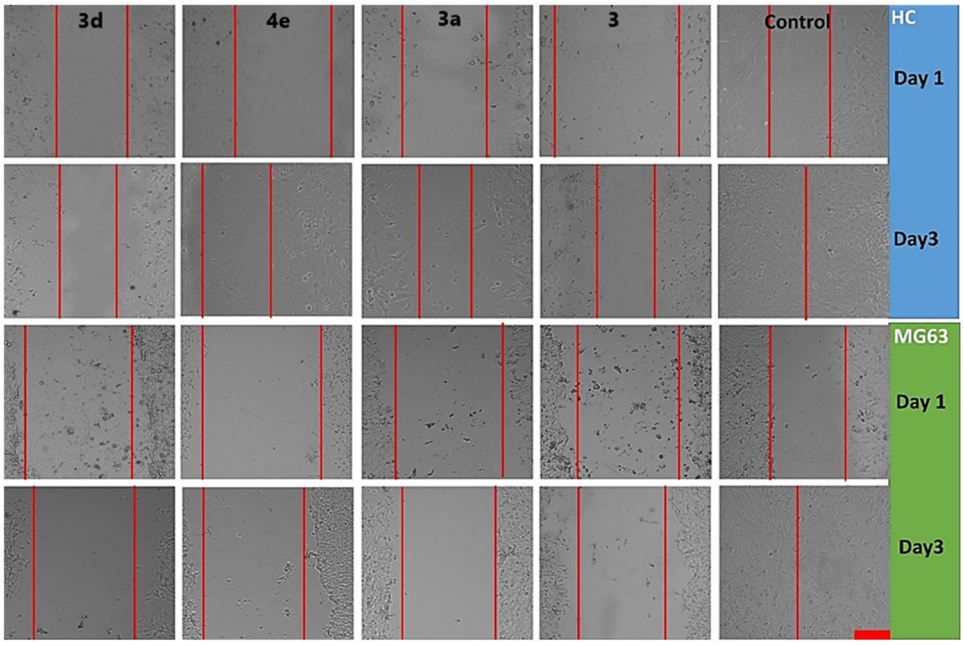


**FIGURE 6** Effects of **3d**, **4e**, **3a**, and **3** on cell migration on HC and MG63 cell lines. All scales are 100 µm.

(Well 1), there was no DNA fragmentation, and intact genomic DNA remained near the well. Overall, it can be inferred that the novel tacrine derivatives may trigger an apoptotic cascade within the cell, leading to the appearance of apoptotic DNA fragmentation.

### 3.2.5 | Effect of substances on cell migration

Cell migration rate is a critical determinant of cancer cells and is a target of interest in the development of new anticancer agents. The ability of cancer cells to migrate plays a key role in their evasion of apoptosis, and migration, along with angiogenesis and invasion, is a crucial step in the metastatic process. Therefore, one of the primary objectives in the development of novel arylated tacrine derivatives is to significantly reduce the migration capacity of cancer cells.

The results of migration tests for compounds **3d**, **4e**, **3a**, and **3** used during the study are as follows. According to the time-dependent migration tests, when these compounds were employed at the TGI concentration, they significantly suppressed the

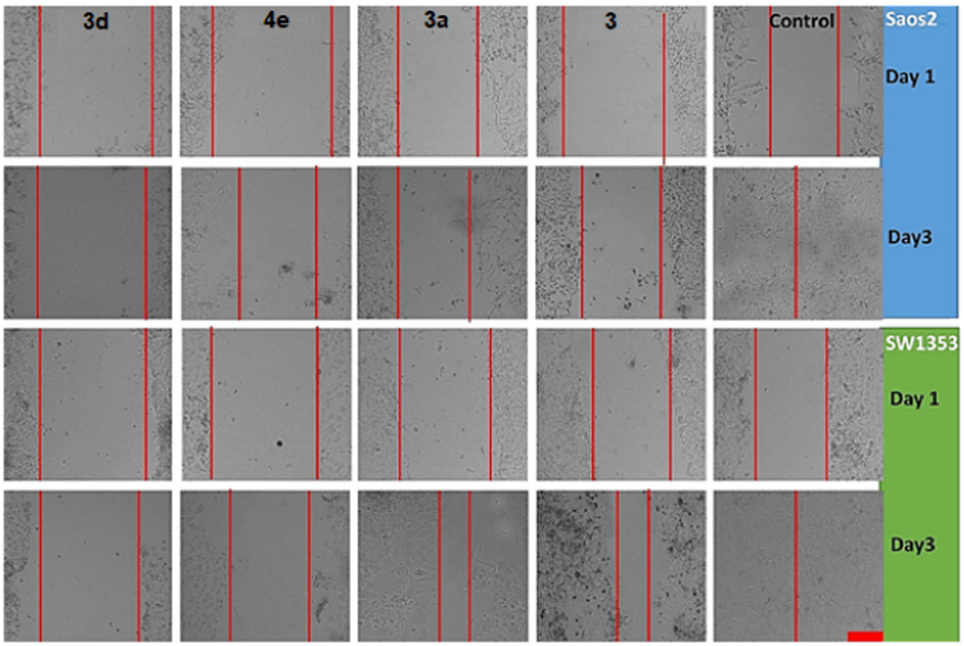


**FIGURE 7** Effects of **3d**, **4e**, **3a**, and **3** on cell migration on Saos2 and SW13536 cell lines. All scales are 100 μm.

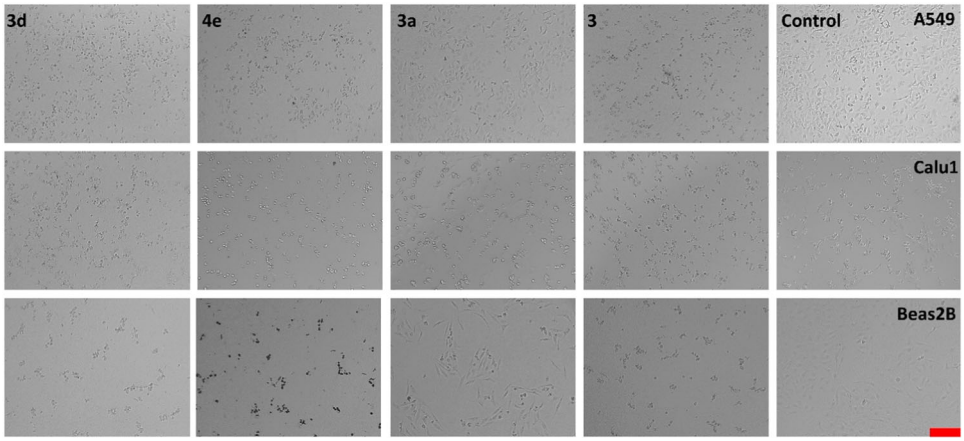


**FIGURE 8** Effect of tested molecules (**3d**, **4e**, **3a** and **3**) on the morphology of A549, Calu1, and Beas2B cell lines. Dimethyl sulfoxide-treated cells as controls. All scale bars show 100 μm.

migration capacity of cancer cells (A549, Calu1, MG63, Saos2, and SW1353) in comparison to control cells (Figures 4–7). However, their ability to suppress migration in normal cells (Beas2B, FL, and HC) was somewhat limited in comparison to their effect on cancer cells (Figures 3–5). With increased incubation time during this test, it became evident that while the control group continued to grow in a linear fashion, unique to cancer cells, the spaces in the insert were not filled in the groups where the test compounds were applied.

According to these test results, as Compounds **3**, **3a**, **3d**, and **4e** demonstrate the inhibition of cell migration, it is likely that the antimetastatic effects of these compounds partly contribute to their anticancer activities.

### 3.2.6 | Effect of the new molecules on cell morphology

In this study, the morphological effects of Compounds **3d**, **4e**, **3a**, and **3** on various cancer cell lines, including lung cancer cells (A549 and Calu1), gynecologic cancer cells (HeLa, A2780, and A2780ADR), colon cancer cells (SW620 and HT29), bone cancer cells (Saos2 and SW1353), as well as normal lung cells (Beas2B), normal chondrocyte cells (HC), and normal epithelial cells (FL), were observed and photographed 24 h after application. The observed morphological alterations were apparent in all cell lines treated with these compounds. Some of the observed changes included weak cell attachment or floating cells, cell aggregation, cell rounding, granular

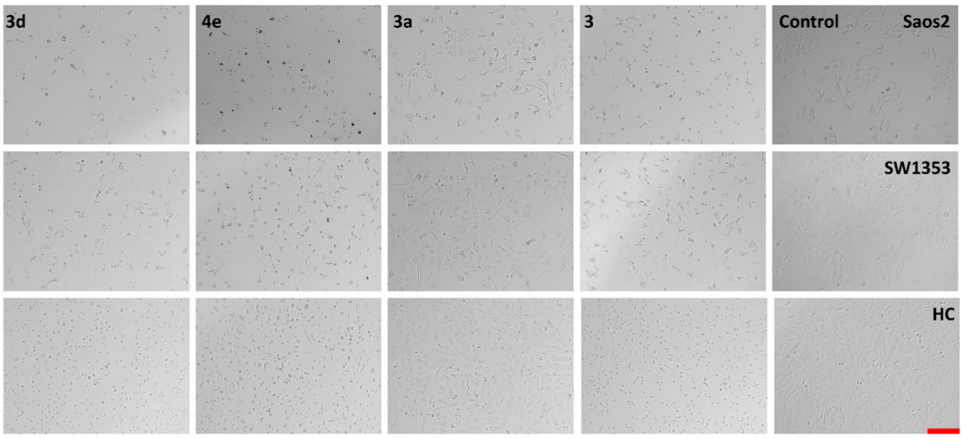


**FIGURE 9** Effect of tested molecules (**3d**, **4e**, **3a**, and **3**) on the morphology of Saos2, SW1353, and HC cell lines. Dimethyl sulfoxide-treated cells as controls. All scale bars show 100 μm.

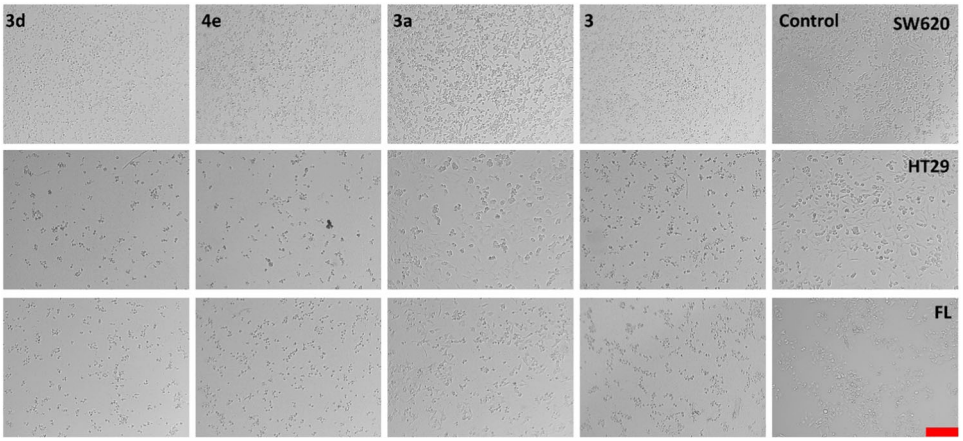


**FIGURE 10** Effect of tested molecules **3d**, **4e**, **3a** and **3**) on the morphology of SW620, HT29, and FL cell lines. Dimethyl sulfoxide-treated cells as controls. All scale bars show 100 μm.

formation, cell blebbing, cellular shrinkage, and the disintegration of cell clumps (Figures 8–11).

The changes in cell morphology resulting from the application of TGI doses of Compounds **3d**, **4e**, **3a**, and **3** indicate that the mechanism of action of these novel tacrine derivatives, including apoptosis, aligns with the results obtained from the MTT assay, DNA degradation assay, and cell migration tests for these compounds (**3d**, **4e**, **3a**, and **3**).

## 3.3 | Evaluation of enzyme inhibitory effects of novel tacrine derivatives (3a–e and 4a–e) against hCA I and hCA II

Based on the test results, the compounds were evaluated for their inhibitory activity against two isoforms of hCA. The $IC_{50}$ values represent the concentration of the compound required to inhibit enzyme activity by 50%, whereas the $K_i$ values represent the binding affinity of the compound for the enzyme.

It is evident that Compounds **3c**, **3d**, and **4e** exhibited strong inhibition of both hCA I and hCA II, with $IC_{50}$ values ranging between 0.572 and 0.824 μM. This is particularly noteworthy when compared to the control compound acetazolamide (AZA) ($IC_{50}$ = 0.633 μM for hCA I and $IC_{50}$ = 0.868 μM for hCA II). On the other hand, Compounds **3b** and **4c** displayed selective inhibitory potential against hCA II, with $IC_{50}$ values of 0.707 and 0.391 μM, respectively.

The test results indicate that Compounds **3c**, **3d**, and **4e** are effective inhibitors of the hCA I enzyme, with $IC_{50}$ values of 0.619, 0.616, and 0.542 μM, respectively. However, Compounds **3a–b**, **3e**, and **4a–d** exhibited weaker inhibitory potential against hCA I, with $IC_{50}$ values ranging between 0.771 and 1.428 μM, which are less effective than the control compound AZA with an $IC_{50}$ value of 0.633 μM.

In contrast, Compounds **3b–d**, **4c**, and **4d** demonstrated significant inhibition of hCA II, with $IC_{50}$ values of 0.707, 0.824, 0.607, 0.391, and 0.693 μM, respectively. Notably, Compound **4c** exhibited the strongest inhibition of hCA II ($IC_{50}$ = 0.391 μM), whereas its inhibition of hCA I ($IC_{50}$ = 0.771 μM) was moderate (Table 6).

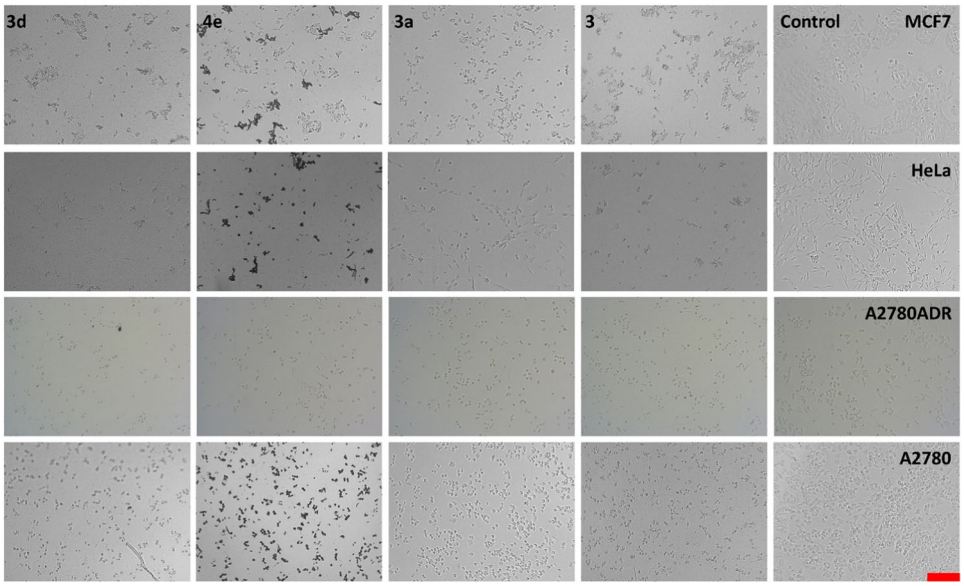


**FIGURE 11** Effect of tested molecules **3d**, **4e**, **3a**, and **3** on the morphology of MCF7, HeLa, A2780ADR, and A2780 cell lines. Dimethyl sulfoxide-treated cells as controls. All scale bars show 100 μm.

**TABLE 6** $IC_{50}$ values of tested compounds (3a–e and 4a–e) against hCA I and II.

| Compounds | IC50 (μM) hCA I | $r^2$ | hCA II | $r^2$ |
|---|---|---|---|---|
| **3a** | 1.428 | 0.8160 | 1.325 | 0.9618 |
| **3b** | 1.209 | 0.9692 | 0.707 | 0.9643 |
| **3c** | 0.619 | 0.9003 | 0.824 | 0.8623 |
| **3d** | 0.616 | 0.9323 | 0.607 | 0.9425 |
| **3e** | 0.971 | 0.9868 | 0.977 | 0.9839 |
| **4a** | 1.074 | 0.9850 | 1.174 | 0.9314 |
| **4b** | 1.193 | 0.9538 | 1.062 | 0.9783 |
| **4c** | 0.771 | 0.9490 | 0.391 | 0.8712 |
| **4d** | 0.838 | 0.9991 | 1.401 | 0.9389 |
| **4e** | 0.572 | 0.9248 | 0.693 | 0.9758 |
| **AZA** | 0.633 | 0.9195 | 0.868 | 0.9914 |

Abbreviations: AZA, acetazolamide; $IC_{50}$, half-maximal inhibitory concentration.

## 3.4 | Evaluation of antibacterial and antifungal effects of of novel tacrine derivatives (3a–e and 4a–e)

The impact of recently synthesized compounds on pathogenic bacteria causing human diseases has been assessed using the MIC method. Employing the MIC values of contemporary antimicrobial drugs as a benchmark, our test molecules were considered antibacterial when demonstrating MIC values of 256 μg/mL or below. Analysis of MIC values against Gram-positive (Gram [+]) and Gram-negative (Gram [−]) bacteria revealed compelling findings.

In Table 7, the antibacterial effects of **3e** against all strains (<4–8 μg/mL) were equal to or surpassed the SCF antibiotic, employed as a positive control. Compound **3d** exhibited antibacterial effects against *E. coli* ATCC 25922 (8 μg/mL) at a level comparable to the SCF antibiotic. Examination of MIC values on bacteria demonstrated that Compounds **3a**, **3c–d**, **4a–b**, and **4d–e** (16–64 μg/mL) exhibited significant antibacterial efficacy (Table 7).

However, Compounds **4c** and **3b** were ineffective against all bacteria (128–256 μg/mL), with exceptions for *S. aureus* and *S. aureus* MSSA (64 μg/mL for **4c**) (Table 8). The original Compounds **3–6** displayed weak antibacterial and antifungal effects (128–>512 μg/mL) (Table 8). Evaluation of MIC values against fungi revealed that all compounds against *C. albicans* ATCC 10231 (256–>512 μg/mL) demonstrated moderate efficacy compared to the FLZ antifungal used as a positive control (Tables 7 and 8).

Notably, Compound **3e** emerged as an exceptional antibacterial agent against *S. gordonii* (<4 μg/mL), a bacteria associated with tooth decay. Furthermore, 5,7-bis(4-(trifluoromethoxy)phenyl)tacrine (**3e**) exhibited potent inhibition against all Gram (+) and Gram (−) bacteria with an MIC value of 8 μg/mL.

Although Compounds **3–6** displayed inefficacy in inhibiting microorganisms, derivatives **3a**, **3c–e**, **4a–b**, and **4d–e**, derived from **3** and **4**, showcased significant inhibitory potential against both Gram (+) and Gram (−) bacteria with MIC values ranging between 4 and 64 μg/mL. These findings suggest that the substitution of the tacrine ring at C-5 and C-7 positions (**3a**, **3c–e**) augmented antibacterial activity. Specifically, tacrine (**3e**) demonstrated enhanced antibacterial properties compared to the starting material **3**, attributed to the presence of a 4-trifluoromethoxyphenyl group at C-5 and C-7.

**TABLE 7** MICs (in μg/mL) of compounds.

| Microorganisms | | 3a | 3b | 3c | 3d | 3e | 4a | 4b | 4c | 4d | 4e |
|---|---|---|---|---|---|---|---|---|---|---|---|
| *Enterococcus faecalis* **VRE** | ATCC 19433 | 64 | 256 | 32 | 16 | 8 | 32 | 64 | 128 | 64 | 32 |
| *E. faecalis* | ATCC 29212 | 64 | 256 | 32 | 16 | 8 | 32 | 64 | 128 | 64 | 64 |
| *Staphylococcus aureus* | ATCC 25923 | 32 | 256 | 32 | 16 | 8 | 32 | 64 | 64 | 32 | 16 |
| *S. aureus* **MSSA** | ATCC 29213 | 64 | 256 | 64 | 16 | 8 | 32 | 64 | 64 | 32 | 16 |
| *S. aureus* **MRSA** | ATCC 46300 | 32 | 256 | 64 | 16 | 8 | 32 | 64 | 128 | 64 | 32 |
| *Escherichia coli* | ATCC 25922 | 64 | 256 | 64 | 8 | 8 | 32 | 64 | 128 | 64 | 64 |
| *Pseudomonas aeruginosa* **AGME** | ATCC 27853 | 64 | 256 | 32 | 16 | 8 | 32 | 64 | 128 | 64 | 32 |
| *Streptococcus gordonii* | NCTC 7870 | 32 | 256 | 32 | 16 | <4 | 32 | 64 | 128 | 64 | 16 |
| *Aggregatibacter actinomycetemcomitans* | ATCC 33384 | 64 | 256 | 64 | 64 | 8 | 64 | 64 | 128 | 64 | 32 |
| *Candida albicans* | ATCC 10231 | 512 | 512 | 512 | 256 | 256 | 512 | 512 | >512 | >512 | 256 |

*Note*: S/CF and FLZ are positive control for bacteria and fungi, respectively.

Abbreviations: AGME, aminoglycoside-modifying enzyme; FLZ, fluconazole; MIC, minimum inhibitory concentration; MRSA, methicillin-resistant *S. aureus*; MSSA, meticillin-sensitive *S. aureus*; S/CF, sulbactam/cefoperazone; VRE, vancomycin-resistant enterococci.

**TABLE 8** MICs (in μg/mL) of compounds.

| Microorganisms | | 3 | 4 | 5 | 6 | Control |
|---|---|---|---|---|---|---|
| *Enterococcus faecalis* **VRE** | ATCC 19433 | 256 | 256 | 256 | 256 | 8 |
| *E. faecalis* | ATCC 29212 | 256 | 256 | 256 | 256 | 4 |
| *Staphylococcus aureus* | ATCC 25923 | 128 | 128 | 256 | 256 | 4 |
| *S. aureus* **MSSA** | ATCC 29213 | 256 | 256 | 256 | 256 | 8 |
| *S. aureus* **MRSA** | ATCC 46300 | 256 | 256 | 256 | 256 | 8 |
| *Escherichia coli* | ATCC 25922 | 256 | 256 | 256 | 256 | 4 |
| *Pseudomonas aeruginosa* **AGME** | ATCC 27853 | 256 | 256 | 256 | 256 | 8 |
| *Streptococcus gordonii* | NCTC 7870 | 256 | 256 | 256 | 256 | 4 |
| *Aggregatibacter actinomycetemcomitans* | ATCC 33384 | 256 | 256 | 256 | 256 | 4 |
| *Candida albicans* | ATCC 10231 | >512 | >512 | >512 | >512 | 64 |

*Note*: S/CF and FLZ are positive control for bacteria and fungi, respectively.

Abbreviations: AGME, aminoglycoside-modifying enzyme; FLZ, fluconazole; MIC, minimum inhibitory concentration; MRSA, methicillin-resistant *Staphylococcus aureus*; MSSA, meticillin-sensitive *Staphylococcus aureus*; S/CF, sulbactam/cefoperazone; VRE, vancomycin-resistant enterococci.

However, the addition of a 4-ethylphenyl group to the tacrine ring (**3b**) did not positively impact antibacterial properties (Tables 7 and 8).

The incorporation of phenyl, 4-ethylphenyl, 4-thiomethylphenyl, and 4-trifluoromethoxyphenyl at C-2 and C-4 positions of tacrines (**4a–b**, **4d–e**), along with a seven membered aliphatic carbon ring similar to the six membered derivatives (**3a–e**), significantly enhanced antibacterial properties compared to the starting material (**4**) (Tables 7 and 8). However, the 4-methoxyphenyl group (**4c**) remained inactive.

## 4 | CONCLUSION

This study was dedicated to the synthesis and assessment of novel diaryl substituted tacrine derivatives for their potential in anticancer and antibacterial activities and enzyme inhibition. The chemical synthesis of diarylated tetrahydroacridines was successfully accomplished through a two-step process involving the Friedlander reaction and the Suzuki–Miyaura cross-coupling reaction, yielding moderate yields. The structures of these compounds were verified through a comprehensive analysis, including NMR and mass spectrometry.

The novel tacrine derivatives **3a–e** and **4a–e** was evaluated their impact on various cancer cell lines. These compounds (**3a–e** and **4a–e**) displayed potent antiproliferative activity against lung, gynecologic, bone, and colon cancer cell lines, with $GI_{50}$ and TGI values falling within the desired range. Notably, two compounds, namely, 2,4-bis(4-(trifluoromethoxy)phenyl)−7,8,9,10-tetrahydro-6H-cyclohepta[b]quinolin-11-amine (**4e**) and 6,8-dibromotacrine (**3**), demonstrated promising results with low cytotoxicity in normal cell lines and potent antiproliferative effects in various cancer cell lines. These findings indicate their potential

for further preclinical studies as cancer-specific treatments. Furthermore, the cytotoxicity assessment revealed that these novel compounds exhibited low cytotoxicity at their TGI concentrations for both normal and cancer cell lines, underscoring their favorable safety profile. On the other hand, novel tacrine analogs displayed specific enzyme inhibition against hCA I and hCA II enzymes. The Compounds **3c**, **3d**, and **4e** exhibited strong inhibition of both hCA I and hCA II, with lower $IC_{50}$ values, compared with control compound, AZA. Additionally, the novel arylated tacrine compounds showed good antimicrobial activity against several Gram (+) and Gram (−) bacteria strains. Especially, Compound **3e** inhibited all tested strains in low MIC values.

In summary, the synthesized diarylated tacrine derivatives (**3a–e** and **4a–e**) have exhibited remarkable anticancer potential, characterized by their selectivity for cancer cells and minimal cytotoxicity in normal cell lines. These results indicate that these compounds hold great promise for further development as potential anticancer and antibacterial agents. Additional investigations are needed to elucidate their mechanisms of action and optimize their effectiveness. This study contributes to the ongoing endeavors in the search for novel and effective therapeutic agents in the field of cancer treatment. It offers valuable insights into the development of promising agents for combating cancer, epilepsy and bacterial.

## AUTHOR CONTRIBUTIONS

**Büşra A. Mısır**: Data curation, writing—original draft, investigation. **Yavuz Derin**: Investigation, writing—original draft, data curation. **Salih Ökten**: Conceptualization, investigation, funding acquisition, writing—original draft, methodology, writing—review and editing, project administration, data curation, supervision. **Ali Aydın**: Data curation, writing—original draft. **Ümit M. Koçyiğit**: Data curation, conceptualization. **Hatice Şahin**: Data curation. **Ahmet Tutar**: Supervision, conceptualization, methodology.

## ACKNOWLEDGMENTS

This study was supported by the Turkish Health Institutes (TUSEB A-Project No: 24138) and TUBITAK 2209-A Program (Project No: 1919B012106356). Büşra A. Mısır is supported by the Council of Higher Education (CoHE) of Turkey with 100/2000 PhD Scholarship.

## DATA AVAILABILITY STATEMENT

Data sharing is not applicable to this article as no new data were created or analyzed in this study.

## REFERENCES

[1] P. N. Kalaria, S. C. Karad, D. K. Raval, *Eur. J. Med. Chem.* **2018**, *158*, 917. https://doi.org/10.1016/j.ejmech.2018.08.040

[2] R. Kasımoğulları, M. Bülbül, B. S. Arslan, B. Gökçe, *Eur. J. Med. Chem.* **2010**, *45*(11), 4769. https://doi.org/10.1016/j.ejmech.2010.07.041

[3] B. S. Arslan, Y. Derin, B. A. Mısır, S. Kaya, İ. Şişman, A. Tutar, M. Nebioğlu, *J. Mol. Struct.* **2022**, *1267*, 133608. https://doi.org/10.1016/j.molstruc.2022.133608

[4] T. Rohand, H. B. El Ayouchia, H. Achtak, A. Ghaleb, Y. Derin, A. Tutar, K. Tanemura, *J. Biomol. Struct. Dyn.* **2022**, *40*, 11837. https://doi.org/10.1080/07391102.2021.1965031

[5] Y. Derin, B. S. Arslan, B. A. Mısır, İ. Şişman, M. Nebioğlu, A. Tutar, *Chem. Heterocycl. Compds.* **2020**, *56*, 1542. https://doi.org/10.1007/s10593-020-02847-6

[6] Ü. M. Koçyiğit, S. Ökten, O. Çakmak, G. Burhan, M. Ataş, P. Taslimi, İ. Gülçin, *ChemistrySelect* **2022**, *7*, e202203469. https://doi.org/10.1002/slct.202203469

[7] S. Ökten, A. Aydin, A. Tutar, *Sakarya Univ. J. Sci.* **2019**, *23*, 824. https://doi.org/10.16984/saufenbilder.469273

[8] S. Ökten, A. Aydın, S. Erkan, A. Tutar, *Lett. Drug Des. Discovery* **2024**, *21*(1), 143. https://doi.org/10.2174/1570180820666230201144615

[9] I. Schmidt, G. Pradel, L. Sologub, A. Golzmann, C. J. Ngwa, A. Kucharski, T. Schirmeister, U. Holzgrabe, *Bioorg. Med. Chem.* **2016**, *24*, 3636. https://doi.org/10.1016/j.bmc.2016.06.003

[10] J. Jeřábek, E. Uliassi, L. Guidotti, J. Korábečný, O. Soukup, V. Sepsova, M. Hrabinova, K. Kuča, M. Bartolini, L. E. Peña-Altamira, S. Petralla, B. Monti, M. Roberti, M. L. Bolognesi, *Eur. J. Med. Chem.* **2017**, *127*, 250. https://doi.org/10.1016/j.ejmech.2016.12.048

[11] J. Janockova, J. Korabecny, J. Plsikova, K. Babkova, E. Konkolova, D. Kucerova, J. Vargova, J. Koval, R. Jendzelovsky, P. Fedorocko, J. Kasparkova, V. Brabec, J. Rosocha, O. Soukup, S. Hamulakova, K. Kuca, M. Kozurkova, *J. Enzyme Inhib. Med. Chem.* **2019**, *34*, 877. https://doi.org/10.1080/14756366.2019.1593159

[12] E. Konkoľová, M. Hudáčová, S. Hamuľaková, R. Jendželovský, J. Vargová, J. Ševc, P. Fedoročko, M. Kožurková, *Molecules* **2021**, *26*(4), 1133. https://doi.org/10.3390/molecules26041133

[13] S. Agatonovic-Kustrin, C. Kettle, D. W. Morton, *Biomed. Pharmacother.* **2018**, *106*, 553. https://doi.org/10.1016/j.biopha.2018.06.147

[14] T. J. Eckroat, D. L. Manross, S. C. Cowan, *Int. J. Mol. Sci.* **2020**, *21*(17), 5965. https://doi.org/10.3390/ijms21175965

[15] S. Ökten, M. Ekiz, Ü. M. Koçyiğit, A. Tutar, İ. Çelik, M. Akkurt, F. Gökalp, P. Taslimi, İ. Gülçin, *J. Mol. Struct.* **2019**, *1175*, 906. https://doi.org/10.1016/j.molstruc.2018.08.063

[16] S. Okten, M. Ekiz, A. Tutar, B. Butun, U. M. Kocyigit, G. Topcu, İ. Gülcin, *Ind. J. Pharm. Educ. Res.* **2019**, *53*(2), 268. https://doi.org/10.5530/ijper.53.2.35

[17] S. Ökten, A. Aydın, Ü. M. Koçyiğit, O. Çakmak, S. Erkan, C. A. Andac, P. Taslimi, İ. Gülçin, *Arch. Pharm. (Weinheim)* **2020**, *353*(9), e2000086. https://doi.org/10.1002/ardp.202000086

[18] A. Aydın, S. Ökten, S. Erkan, M. Bulut, E. Özcan, A. Tutar, T. Eren, *ChemistrySelect* **2021**, *6*(13), 3286. https://doi.org/10.1002/slct.202004753

[19] Z. Solárová, M. Kello, S. Hamuľaková, L. Mirossay, P. Solár, *Acta Chim. Slov.* **2018**, *65*, 875. https://doi.org/10.17344/acsi.2018.4519

[20] T. B. Ferguson, S. O. Thorne Jr., *J. Pharmacol. Exp. Ther.* **1946**, *86*(3), 258.

[21] M. Ekiz, A. Tutar, S. Ökten, *Tetrahedron* **2016**, *72*, 5323. https://doi.org/10.1016/j.tet.2016.07.012

[22] C. Derabli, I. Boualia, A. B. Abdelwahab, R. Boulcina, C. Bensouici, G. Kirsch, A. Debache, *Bioorg. Med. Chem. Lett.* **2018**, *28*, 2481. https://doi.org/10.1016/j.bmcl.2018.05.063

[23] H. Bekolo, G. Kirsch, *Can. J. Chem.* **2007**, *85*, 1. https://doi.org/10.1139/V06-180

[24] A. M. Salaheldin, A. M. F. Oliveira-Campos, P. Parpot, L. M. Rodrigues, M. M. Oliveira, F. P. Feixoto, *Helv. Chim. Acta* **2010**, *93*, 242. https://doi.org/10.1002/hlca.200900190

[25] J. Marco-Contelles, R. León, C. De Los Ríos, A. Samadi, M. Bartolini, V. Andrisano, O. Huertas, X. Barril, F. J. Luque, M. I. Rodríguez-Franco, B. López, M. G. López, A. G. García, M. do Carmo Carreiras, M. Villarroya, *J. Med. Chem.* **2009**, *52*, 2724. https://doi.org/10.1021/jm801292b

[26] D. Thomae, E. Perspicace, S. Hesse, G. Kirsch, P. Seck, *Tetrahedron* **2008**, *64*, 9309. https://doi.org/10.1016/j.tet.2008.07.017

[27] M. Eghtedari, Y. Sarrafi, H. Nadri, M. Mahdavi, A. Moradi, F. Homayouni Moghadam, S. Emami, L. Firoozpour, A. Asadipour, O. Sabzevari, A. Foroumadi, *Eur. J. Med. Chem.* **2017**, *128*, 237. https://doi.org/10.1016/j.ejmech.2017.01.042
[28] Y. Dgachi, O. Sokolov, V. Luzet, J. Godyń, D. Panek, A. Bonet, H. Martin, I. Iriepa, I. Moraleda, C. García-Iriepa, J. Janockova, L. Richert, O. Soukup, B. Malawska, F. Chabchoub, J. Marco-Contelles, L. Ismaili, *Eur. J. Med. Chem.* **2017**, *126*, 576. https://doi.org/10.1016/j.ejmech.2016.11.050
[29] M. M. Badran, M. A. Hakeem, S. M. Abuel-Maaty, A. El-Malah, R. M. A. Salam, *Arch. Pharm. (Weinheim)* **2010**, *343*, 590. https://doi.org/10.1002/ardp.200900226
[30] J. M. Roldán-Peña, V. Romero-Real, J. Hicke, I. Maya, A. Franconetti, I. Lagunes, J. M. Padron, S. Petralla, E. Poeta, M. Naldi, M. Bartolini, B. Monti, M. L. Bolognesi, O. Lopez, J. G. Fernandez-Bolanos, *Eur. J. Med. Chem.* **2019**, *181*, 111550. https://doi.org/10.1016/j.ejmech.2019.07.053
[31] E. Riazimontazer, H. Sadeghpour, H. Nadri, A. Sakhteman, T. T. Küçükkılınç, R. Miri, N. Edraki, *Bioorg. Chem.* **2019**, *89*, 103006. https://doi.org/10.1016/j.bioorg.2019.103006
[32] C. Zhang, Q. Y. Du, L. D. Chen, W. H. Wu, S. Y. Liao, L. H. Yu, X. T. Liang, *Eur. J. Med. Chem.* **2016**, *116*, 200. https://doi.org/10.1016/j.ejmech.2016.03.077
[33] S. Codony, C. Pont, C. Griñán-Ferré, A. Di Pede-Mattatelli, C. Calvó-Tusell, F. Feixas, S. Osuna, J. Jarné-Ferrer, M. Naldi, M. Bartolini, M. I. Loza, J. Brea, B. Pérez, C. Bartra, C. Sanfeliu, J. Juárez-Jiménez, C. Morisseau, B. D. Hammock, M. Pallàs, S. Vázquez, D. Muñoz-Torrero, *J. Med. Chem.* **2022**, *65*, 4909. https://doi.org/10.1021/acs.jmedchem.1c02150
[34] A. Babu, M. N. Joy, K. Sunil, A. M. Sajith, S. Santra, G. V. Zyryanov, O. A. Konovalova, I. I. Butorin, K. Muniraju, *RSC Adv.* **2022**, *12*, 22476. https://doi.org/10.1039/d2ra03225b
[35] E. K. Reddy, C. Remya, K. Mantosh, A. M. Sajith, R. V. Omkumar, C. Sadasivan, S. Anwar, *Eur. J. Med. Chem.* **2017**, *139*, 367. https://doi.org/10.1016/j.ejmech.2017.08.013
[36] S. Ökten, *J. Chem. Res.* **2019**, *43*(7–8), 274. https://doi.org/10.1177/1747519819861389
[37] R. F. Yilmaz, Y. Derin, B. A. Misir, V. E. Atalay, Ö. F. Tutar, S. Ökten, A. Tutar, *J. Mol. Struct.* **2023**, *1291*, 135962. https://doi.org/10.1016/j.molstruc.2023.135962
[38] Y. Kabri, M. D. Crozet, T. Terme, P. Vanelle, *Eur. J. Org. Chem.* **2015**, *2015*, 3806. https://doi.org/10.1002/ejoc.201500162
[39] D. D. Perrin, W. L. Armarego, D. R. Perrin, *Purification of laboratory chemicals*, Butterworth-Heinemann, Oxford **1988**.
[40] T. Mosmann, *J. Immunol. Methods* **1983**, *65*(1–2), 55. https://doi.org/10.1016/0022-1759(83)90303-4
[41] T. Decker, M. L. Lohmann-Matthes, *J. Immunol. Methods* **1988**, *115*, 61. https://doi.org/10.1016/0022-1759(88)90310-9
[42] R. K. Emaus, R. Grunwald, J. J. Lemasters, *Biochim. Biophys. Acta Bioenergetics* **1986**, *850*, 436. https://doi.org/10.1016/0005-2728(86)90112-X
[43] J. P. Gong, F. Traganos, Z. Darzynkiewicz, *Anal. Biochem.* **1994**, *218*, 314. https://doi.org/10.1006/abio.1994.1184
[44] J. A. Verpoorte, S. Mehta, J. T. Edsall, *J. Biol. Chem.* **1967**, *242*, 4221. https://doi.org/10.1016/S0021-9258(18)95800-X

## SUPPORTING INFORMATION

Additional supporting information can be found online in the Supporting Information section at the end of this article.

**How to cite this article:** B. A. Mısır, Y. Derin, S. Ökten, A. Aydin, Ü. M. Koçyiğit, H. Şahin, A. Tutar, *J. Biochem. Mol. Toxicol.* **2024**, *38*, e23706. https://doi.org/10.1002/jbt.23706